Analysis of Myosin XI Localization During Cell Division in *Physcomitrella patens*

By

Hao Sun

A Thesis

Submitted to the Faculty

Of The

WORCESTER POLYTECHNIC INSTITUTE

In partial fulfillment of the requirement for the

Degree of Master of Science

In

Biology & Biotechnology

Spring 2015

Approved:

_____	_____
Dr. Luis Vidali, Ph.D. Major Advisor – WPI	Dr. David S. Adams, Ph.D. Committee Member - WPI
_____	
Dr. Samuel M. Politz, Ph.D. Committee Member - WPI	

ABSTRACT

Cell division is an important biological process, thus it is always an active field in biological research. To complete cell division, plant cells form a new cell wall that separates the two new cells. In contrast to the contractile ring of animal cells, plant cells form the new cell wall from their interior. Vesicles containing the new cell wall fuse at the cell plate between the two cells. The formation of the cell plate is guided by the phragmoplast, a microtubule and filamentous actin-containing structure. Because vesicles are known to be transported by myosin motors during interphase and little is known about the role of myosin XI during cell division, I investigated the participation of the plant specific myosin XI in cell division. For this work I used the moss *Physcomitrella patens* as a model organisms because of its simple cytology and powerful genetics. Using a fluorescent protein fusion of myosin XI, I found that this molecule associates with the mitotic spindle immediately after nuclear envelope breakdown. Myosin XI stays associated with the spindle during mitosis, and when the phragmoplast is formed, it concentrates at the cell plate, forming a fine line. Using an actin polymerization inhibitor, latrunculin B, I found that the associations of myosin XI with the mitotic spindle and the phragmoplast are independent of the presence of filamentous actin. After using double-labeled lines for myosin XI the endoplasmic reticulum and vesicle markers, I found the myosin XI on the spindle is not colocalized with the endoplasmic reticulum and two types of vesicle markers. Furthermore, I also found the vesicle trafficking inhibitor, brefeldin A, does not inhibit the localization of myosin XI at the mitotic spindle and the phragmoplast. These observations suggest a new actin-independent behavior of myosin XI during cell division, and provide novel insights to our understanding of the function of myosin XI during plant cell division.

ACKNOWLEDGEMENTS

I am grateful that I received plenty of assistance from people listed below after I joined the Vidali lab, without their help, I might not have bene able to finish this project now.

To begin with, I would like to thank my advisor Dr. Luis Vidali. He is always very patient teaching me how to perform new experiments, as well as to think as a scientific researcher. Throughout my graduate study, he gave me enormous support and encouragement, which make my life in the lab more enjoyable.

I also want to thank the rest of my committee members: Dr. David Adams and Dr. Samuel Politz, who give me many insightful ideas and suggestions about my project. With their help, my project became more interesting and conclusive.

In addition to my committee members, I would like to give my thanks to all the lab members in Vidali lab. In particular, I want to thank Dr. Fabienne Furt and Mr. Jeff Bibeau for teaching me research techniques and for their thoughtful advice about this project. I also want to thank the rest of the lab members for their support and encouragement.

Last but not least, I would like to thank Dr. Arne Gernicke, from the Department of Chemistry and Biochemistry for the use of his Nikon Ti microscope, and the Department of Biology and Biotechnology as well as WPI's Imaging Core for their support during my project.

TABLE OF CONTENTS

TABLE OF FIGURES

TABLE OF ABBREVIATIONS

Abbreviations	Full Name
BDM	2,3-Butanedione monoxime
BFA	Brefeldin A
CDS	Cortical Division Site
DRP	Dynein-Related protein
ER	Endoplasmic Reticulum
F-actin	Filamentous actin
GTP	Guanosine-5'-triphosphate
KRP	Kinesin-Related protein
LatB	Latrunculin B
LINC complex	Linker of Nucleoskeleton and Cytoskeleton complex
MAP	Microtubule-Associated Protein
mEGFP	Monomeric Enhanced Green Fluorescent Protein
MT	Microtubule
MTOC	Microtubule Organizing Center
PPB	Preprophase Band
SH3-like domain	SRC Homology 3-like domain
SIN	Septation Initiation Network
SNARE protein	SNAP Receptor protein
VAMP	Vesicle Associated Membrane Protein

1. INTRODUCTION

One of the most important features of cells is that they can make new copies of themselves by cell division. This is important because all cells arise from pre-existing cells-unicellular organisms use cell division to maintain a reasonable number of individuals in the environment, and multicellular organisms use cell division to generate clusters of cells to form complex structures. Thus, cell division has been a very active research topic since late 19th century.

From years of study, much progress has been made in understanding cell division. For example, in prokaryotic organisms, researchers have found that bacterial cell division needs the formation of an FtsZ ring (Z ring) (Dai and Lutkenhaus, 1991; Lutkenhaus and Addinall, 1997); in eukaryotic organisms, the importance of the formation of the mitotic spindle is well documented and a general idea of how cytokinesis takes place has emerged (Glotzer, 2001; Scholey et al., 2003). Cell division in plants is less understood because most of the existing knowledge about cell division in eukaryotic organisms was done in animal and yeast cells. Though there are many similarities in fundamental mechanisms between plant and animal cell division (Lloyd and Chan, 2006), a number of differences exist, especially in cytokinesis. For instance, in animal and yeast cells, it is known that myosin II is important for cytokinesis (Bezanilla et al., 1997; Gerisch and Weber, 2000; Komatsu et al., 2000), but plant cells have no myosin II or orthologous genes (Thompson and Langford, 2002); and most obviously, plant cells do not form a contractile ring to complete cell division. Instead, they have a structure called the phragmoplast to help separate two daughter cells. Given all these differences, in order to have a better understanding of cell division in plants, more study should be done on the specific structures that define this process.

1.1: Cell Divisions in Other Systems

The majority of the existing research on cell division focuses on four main types of cells: bacterial, fungal, animal and plant.

Evolutionarily, bacterial cell division is thought to be the most primary type of cell division. Cell division in bacterial cells is mainly conducted by a tubulin homologue, Fts Z. Just like tubulin, Fts Z can polymerize into protofilaments in the present of GTP (Bramhill and Thompson, 1994; Erickson et al., 1996; Lu et al., 2000) and these protofilaments will then form a structure called Fts Z ring (Z ring) at the division plane. Researchers have shown mutations in Fts Z may cause severe defects in cell division in bacteria (Bi and Lutkenhaus, 1991; Mukherjee et al., 2001). After the formation of the Fts Z ring, with the help of many other regulators, such as Fts-A and Zip-A (Pichoff and Lutkenhaus, 2002), the bacterial cells constrict the Fts Z (Bramhill, 1997). At the final stage of cell division, bacterial cells form a septum to make the final separation of two daughter cells.

Unlike bacterial cells that use a "microtubule" based ring structure, fungal and animal cells use another type of machinery, the actomyosin-based contractile ring, to physically divide two daughter cells, though the basic idea is the same: form a ring-like structure to constrain the division plane, and when the connection between two cells is small enough, other protein complex-such as the septation initiation network (SIN), will join and regulate the final cut (Furge et al., 1998). The contractile ring in fungal and animal cells is a structure formed with actin filaments and myosin II (Bezanilla et al., 1997; Kitayama et al., 1997; May et al., 1997), along with some regulatory elements, like α-actinin (Mukhina et al., 2007) and formin (Pollard, 2010). With the help of advanced imaging methods, investigators have found the actin filaments in the

contractile rings are oriented in both directions (Schroeder, 1973; Sanger and Sanger, 1980). And myosin II in the contractile rings may also form filaments (Reichl et al., 2008; Zhou and Wang, 2008), indicating that myosin II may generate force in the contractile rings by a mechanism similar to muscles.

When discussing cell division, we are not only indicating the physical segregation of two daughter cells as mentioned above, but in addition, eukaryotic cells have developed a cell division specific structure called mitotic spindle to pull two sets of chromosomes into two daughter cells during cell division. The formation of the mitotic spindle in fungal cells requires another structure called the spindle pole body, and in animal cells requires centrosomes, while plant cells do not have any of these structures to assist their spindle assembly. In the case of animal cells, it is known that centrosomes will be duplicated during S phase (Sluder and Rieder, 1985a, b), and subsequently, animal cells will change the dynamics of their microtubules (Masuda et al., 1988; McNally, 1996; Cassimeris, 1999) via factors like katanin (microtubule severing protein) (McNally and Thomas, 1998), and kin 1 family of kinesin-related protein (Desai et al., 1999). During prometaphase, after nuclear envelope breakdown, microtubules are rapidly assembled from two centrosomes to connect chromosomes at kinetochores.

However, plant cells do not need microtubule organization centers, such as centrosomes, to form the spindles. And they do not need the actomyosin-based contractile rings to complete cytokinesis; instead, they use microtubules to perform this function. Given these key differences, knowledge about other eukaryotic systems is not sufficient for understanding cell division in plant cells. Thus, in the following section, I will briefly summarize what is currently known about cell division in plants.

1.2: Plant Cell Division

1.2.1 Plant Spindle

As mentioned before, most fungal and animal cells have both centrosomes and microtubule motors to help assemble their spindle that function as chromosome separation machinery. But because plant cells do not have centrosomes and one type of microtubule motor, dyneins, the spindle assembly in plants is quite different from fungal and animal spindle assembly (See **Figure I.1**).

Before mitosis starts, plant cells have abundant microtubules surrounding the nuclear envelope (**Fiugre I.1**, lower left panel). These microtubules, also known as perinuclear microtubules, can be formed by two mechanisms (Masoud et al., 2013). One is dependent on **γ**–tubulin ring complexes (**γ**–TuRCs), which is a common microtubule nucleation mechanism whose importance to microtubule nucleation in plant has been confirmed by gene knockdown (Binarova et al., 2006) and knockout experiments (Pastuglia et al., 2003; Nakamura and Hashimoto, 2009). The second mechanism is dependent on histone-1/tubulin complex (Hotta et al., 2007), which is a novel mechanism initially observed in the tobacco cultured cell line BY-2.

During late G_2, the cortical microtubules will form a structure called the preprophase band (which will be discussed later). Meanwhile, the perinuclear microtubules will start accumulating (Kumagai et al., 2001; Dhonukshe et al., 2006) and undergoing conformational changes (Murata and Hasebe, 2007), probably mediated by katanin (Ambrose and Wasteneys, 2008; Panteris et al., 2011). Following this, some microtubule motor proteins will join and work on the microtubules, regulating the organization of these microtubules (Bannigan et al., 2008; Zhu and

Dixit, 2012) and generating tensions on nuclear envelopes (Vos et al., 2000).These microtubules will then invaginate the nuclear envelopes (Dixit and Cyr, 2002).

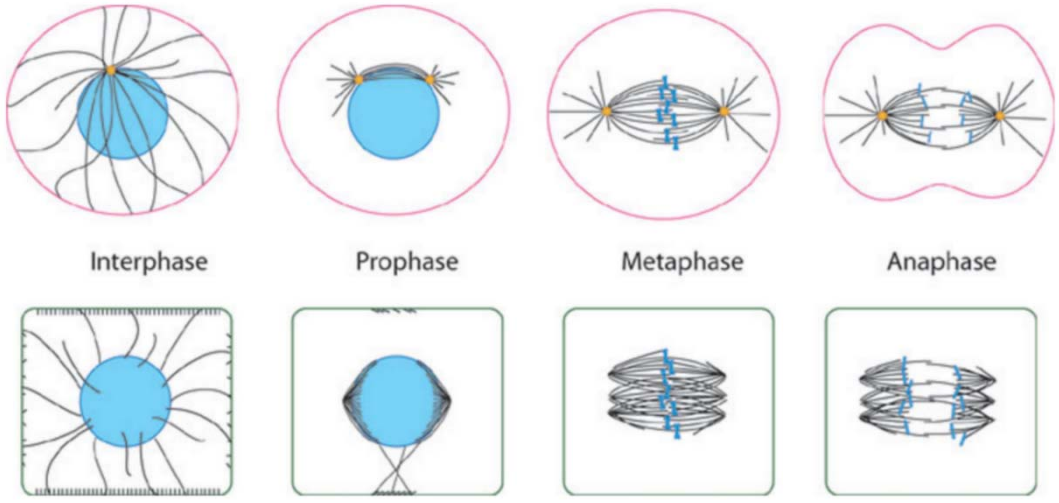

Figure I.1. Comparison of mitotic spindle structure in animals (top) and plants (bottom). From (Bannigan et al., 2008), figure 1.

After the nuclear envelope breaks, microtubules will have another organizational change, and more proteins will participate in spindle formation. For example, many kinesins and kinesin-like proteins (Liu et al., 1996) are found to be important for spindle formation in plants. Knocking-out or mutating the kinesins causes severe defects in spindle formation (Wiedemeier et al., 2002; Bannigan et al., 2007). In addition to these motor proteins, investigators have also identified other important players such as microtubule associated proteins (MAPs) (Fache et al., 2010), the augmin complex (Ho et al., 2011; Hotta et al., 2012; Nakaoka et al., 2012), nucleoporins (Lee et al., 2009), and nuclear envelope-associated proteins (Graumann and Evans, 2011; Oda and Fukuda, 2011), all of which play different roles to ensure proper spindle formation.

During prometaphase, the interpolar microtubules form at the polar regions and pass through the equator, while the kinetochore microtubules grow until they meet chromosomes

(Dhonukshe et al., 2006). However, accumulating evidence suggests there are also microtubules growing from or near the chromosomes (Binarova et al., 1998; Dhonukshe et al., 2006; Zhang and Dawe, 2011).

Currently, many things are known about plant spindle formation and regulation, but many of the ideas are borrowed from animal/yeast studies, and little is known about the details of these processes. Some regulatory components have been identified, but the knowledge of how they come to their target and how they interact with each other is still lacking.

1.2.2 Preprophase Band and Cortical Division Site

As mentioned above, the cortical microtubules, with F-actin and other proteins, form the preprophase band (PPB) during late G_2 phase. The PPB is thought to be important to plant cell division as it can predict the future division site.

To make the transition from the widely distributed localization of cortical microtubules during interphase to the restricted narrow band-distribution of cortical microtubules during preprophase, plant cells may require both the selective depolymerization of non-PPB microtubules (Dhonukshe and Gadella, 2003) and the selective stabilization of PPB microtubules (Vos et al., 2004), which need the assistance of many proteins or protein complexes (Chang-Jie and Sonobe, 1993; Smertenko et al., 2004; Ambrose and Wasteneys, 2008; Gaillard et al., 2008; Kawamura and Wasteneys, 2008; Wright et al., 2009).

The PPB starts disassembling before prometaphase and leaves some marks to guide cytokinesis; hence the location of PPB will define the cortical division site (CDS). Some markers are negative markers, like actin (Hoshino et al., 2003; Panteris, 2008) and a plant kinesin, KCA1 (Vanstraelen et al., 2006) - after the PPB is disassembled, cortical actin and KCA1 will be

depleted only at the CDS, leaving a depleted zone at the CDS. The other markers are positive markers. For example, TAN is found localized at the CDS, and is thought to be important to guide the expansion of the phragmoplast (Cleary and Smith, 1998; Walker et al., 2007); RanGAP1 also localizes to the PPB and remains at the CDS throughout cell division (Xu et al., 2008).

It has been postulated that the function of the CDS is to guide the orientation of the phragmoplast (Muller et al., 2009). One supporting line of evidence is that during telophase, it was found that in both *Arabidopsis* cells and BY-2 cells, microtubules frequently contact the CDS (Chan et al., 2005; Dhonukshe et al., 2005). An alternative function of the CDS might be to promote cell wall maturation, this is supported by experiments where growing cell plates were forced to attach to cell surface other than the CDS, and these new cell walls failed to mature properly (Gunning and Wick, 1985).

Interestingly, the PPB is not formed in the protonemal cells of *P. patens*, but the location of the future cell division site is well regulated in these cells. This suggests that some of the functions performed by the PPB can be accomplished by alternative mechanisms. Though a general idea of PPB and CDS organization has emerged, as well as their possible function during cell division, there is no doubt that more regulatory components need to be identified, and a clearer picture of the relationships between already known players in PPB and CDS is still waiting to be obtained.

1.2.3 Plant Cytokinesis

After the two sets of chromosomes are separated, in plant cells, the phragmoplast assembles in the middle of the plane of division. The phragmoplast is mainly formed by

microtubules that form two antiparallel sets of co-aligned filaments and usually interdigitated in the middle (Hepler and Jackson, 1968; Hiwatashi et al., 2008).

As showed in figure I 2, after the phragmoplast forms, Golgi-derived vesicles start to move in and fuse with each other. Two types of vesicle sizes are found by electron tomography. The larger vesicles are thought to be generated by fusion of smaller ones. The tubulo-vesicular network generated by these fusion events is called the cell plate, which stays in the middle of the two sets of microtubules (Segui-Simarro et al., 2004; Jurgens, 2005a). In order to constrain these vesicles in cell plate, dynamin-related proteins (DRPs) seem to form a ring surrounding the cell plate (shown in **Figure I.2**) (Hong et al., 2001; Otegui et al., 2001). SNARE proteins are also critical for proper cell division, because they mediate membrane fusion of these vesicles. One of these SNARE proteins, called KNOLLE, is found only localized at the cell plate, and mutations of KNOLLE will cause defects in vesicle fusion at the cell plate (Lauber et al., 1997). Similarly, the vesicle SNARES or VAMPs (VAMP 721, 722) are also required for vesicle fusion during cytokinesis (El Kasmi et al., 2013).

After the initiation of the cell plate, the microtubules in the middle of the phragmoplast start depolymerizing while those at the periphery of the cell plate remain stable (Nishihama and Machida, 2001). The depolymerization or destabilization of microtubules in the middle of the phragmoplast is probably caused by the phosphorylation of MAP65, which has a significant reduction of microtubule-bundling activity when phosphorylated (Sasabe et al., 2006; Lee and Liu, 2013). It has been proposed that the phosphorylated MAP65 at the center of the phragmoplast loses its normal function of microtubule bundling, leading to depolymerization of these “unprotected” microtubules (Sasabe et al., 2006; Lee and Liu, 2013). Meanwhile, in order to expand the phragmoplast towards the peripheral cell walls; these microtubules will also need

to be amplified at the periphery. The nucleation of microtubules in the expanding phragmoplast is probably mediated by γ -tubulin and regulated by kinesin 14 (Murata et al., 2013). Thus, the phragmoplast dynamic structure is that of an expanding ring-like array of microtubules, until this array reaches the side membrane of the dividing cells.

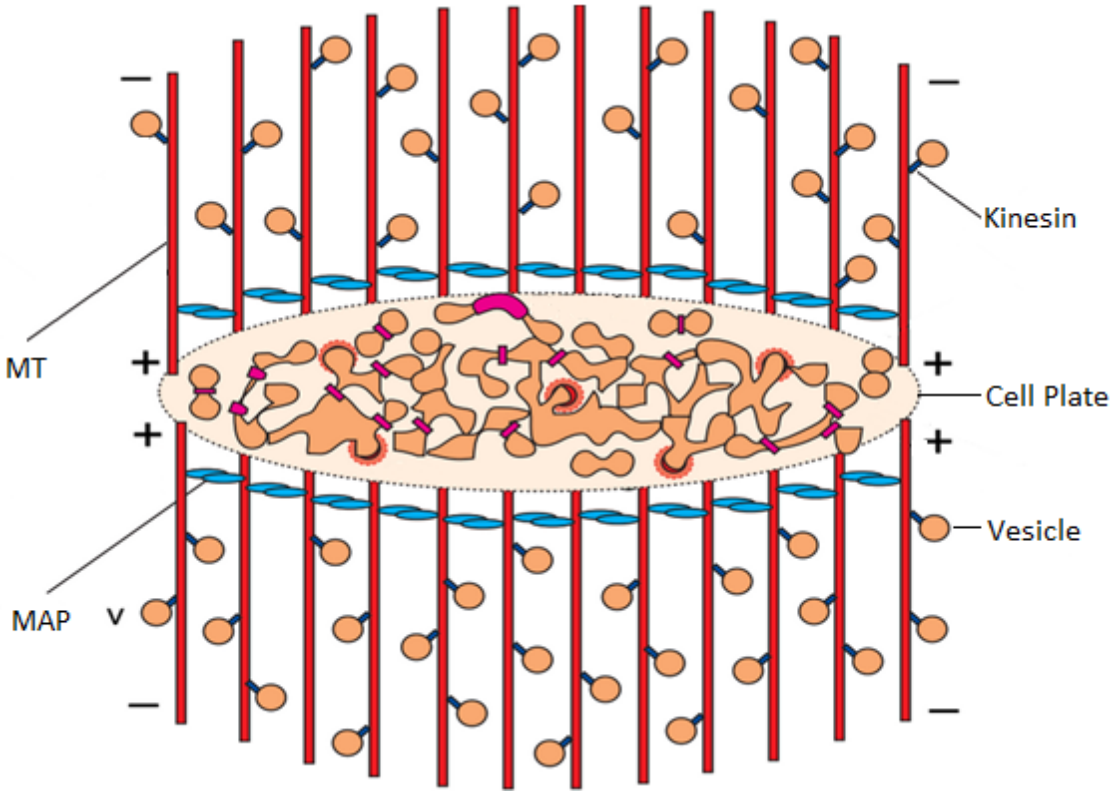

Figure I.2: Cell plate assembly. Modified from (Jurgens, 2005a), figure 2. Vesicles might be transported by kinesin along the phragmoplast microtubules, which is regulated by microtubule associated proteins (MAPs).

In addition to microtubules, actin filaments have also been identified at the phragmoplast, lining up with microtubules (Hepler et al., 2002). The function of these actin filaments is still not clear yet. In fact, experiments with actin inhibitors showed no effect on cell division (Hoshino et al., 2003; Sano et al., 2005), which questions the importance of filamentous actin participating in cytokinesis (Muller et al., 2009).

1.2.4 Comparisons of Cell Division in Animal and Plant Cells

Many differences exist between cell division in animals and plants: animal cells have centrosomes to form spindles, while plants lack these structures; animal cells determine the division site only after the spindle is formed, plants instead create the PPB before the nuclear envelopes break down; animal cells use contractile rings to make a cleavage furrow, while plants form a peripherally expanding phragmoplast to make cell plate.

However, taking a closer look at the cell division in animal and plant cells, many similarities can also be found between these two systems. For example, one major difference between animal and plant cell division is the presence or absence of centrosomes to form the spindle, nevertheless, many similarities exist in terms of spindle formation. In plants, many of the spindle microtubules are nucleated on the chromosomes (Binarova et al., 1998; Dhonukshe et al., 2006; Zhang and Dawe, 2011); similarly, in animal cells, even though they have centrosomes to form the spindle, the nucleation of microtubules on the chromosomes is also important for spindle formation (Gruss et al., 2002; Gadde and Heald, 2004; Maiato et al., 2004). In addition, the kinesin 14 family of motors is important to spindle formation in both animal and plant cells (Sharp et al., 1999; Huisman et al., 2004; Ambrose et al., 2005).

Another example is the similarity between the animal midbody and the plant phragmoplast. They both are localized at the middle of the division plane, both are mainly formed by

microtubules, and both are critical for cytokinesis in animal or plant cells. In addition, in both structures, microtubule bundling proteins are present and are essential for their formation and activity: plant cells have MAP65 (Jurgens, 2005b), while animal cells have the MAP65 homologue, PRC1 (Mollinari et al., 2002).

In summary, though cell divisions in plant and animal cells seem different, similarities exist between these two systems. As a matter of fact, because we know a great deal from studies with animal cells, we can apply some of this knowledge to better understand the less understood plant system.

1.3: Cell Division Studies in *Physcomitrella patens*

The moss *Physcomitrella patens* is a plant model system with many advantages for studying many fundamental biological processes. *P. patens* is easy to grow and propagate, which allows experiments to be done in a relatively short time. The protonema cells, which are the focus of many studies in polarized cell growth, are filaments made by chains of single cells. The cells are transparent, which makes them excellent subjects for microscopical observations. Most moss cells are haploid, which facilitates genetic analysis; furthermore, it is easier to manipulate *P. patens* genes than other plant model systems because of the availability of mitotic homologous recombination. Furthermore, its whole genome sequence is available, which facilitates bioinfomatic analyses. Thus, this model system is increasing its popularity in many laboratories (Schaefer and Zryd, 1997; Bezanilla et al., 2005; Rensing et al., 2008). However, most of the studies with *P. patens* have focused on tip growth. Only a handful of reports in the literature use *P. patens* to study cell division (Hiwatashi et al., 2008; Kosetsu et al., 2013; Hiwatashi et al., 2014; Miki et al., 2014; Wu and Bezanilla, 2014). Among them, only one report

published last year analyzed the relationship between actin, myosin and plant cell division (Wu and Bezanilla, 2014). This work found myosin VIII localized to the *P. patens* mitotic spindle, the phragmoplast and the cortical division site. When cells were treated with the actin-depolymerizing drug, latrunculin B (LatB), the authors were still able to detect the localization of myosin VIII on the spindle and at the phragmoplast, suggesting an actin-independent mechanism for myosin VIII localization. However, they also observed that when treated with LatB, the phragmoplast had defects at the cells that were forming a branch, similar to the defect in myosin VIII null lines, leading them to conclude that the function of myosin VIII may be dependent on actin filaments though the localization of myosin VIII is not. They also analyzed the localization of an actin filament nucleator, a class II formin (For2A) and they found that this molecule accumulates only late on the spindle and remains on the edge of the phragmoplast throughout cytokinesis. Together, these results suggest that myosin VIII might associate with microtubules and work with actin to guide the expansion of the phragmoplast. As plants only have two types of myosins, VIII and XI, it will be important to investigate and compare the localization myosin XI during cell division.

1.4: Myosin, Vesicles and the Endoplasmic Reticulum

1.4.1 Myosins in Plants

Myosin is a large superfamily of proteins that function as motors working on actin filaments. All of them hydrolyze ATP and produce forces along actin filaments. Myosins typically contain three subdomains: the head/motor domain, the neck domain and the tail domain (See **Figure I.3**). The motor domain is the most conserved part of myosin, which can bind actin and ATP, generating force on actin filaments; the neck domain can be considered as the linker -- or lever arm -- between the head domain and the tail domain; it usually contains helical

sequences called IQ motifs, which can bind light chains or calmodulin; the neck domain also works as a regulatory element. The tail domain is the most diverse domain, which in some cases has a coil-coiled based dimerization domain and a globular domain that connects myosins with their cargos (Cope et al., 1996).

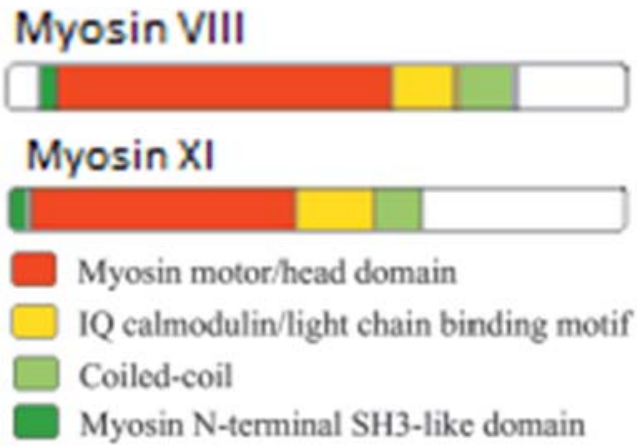

Figure I.3. Domain comparison of myosin VIII and myosin XI. Modified from (Thompson and Langford, 2002).

By the year 2000, researchers had identified as many as 18 different classes of myosin (Furusawa et al., 2000). However, none of these are expressed universally throughout all phyla. Myosin II, for example, is important for animal cell motility and division, while it is not present in plant cells; on the other hand, plants only have the myosin V homologues: myosin VIII and myosin XI (Thompson and Langford, 2002).

Phylogenetic analysis, and the presence of myosin VIII in all land plants suggest that myosin VIII appeared in evolution prior to the radiation of terrestrial plants, but after the divergence of green algae (Thompson and Langford, 2002). Myosin VIII has been implicated in cell plate maturation (Reichelt et al., 1999), intercellular transportation (Baluska et al., 2001;

Avisar et al., 2008; Golomb et al., 2008), and plasmodesmata structure and function (Volkmann et al., 2003).

Another important plant myosin is myosin XI, which is thought to be a homologue to myosin V (Thompson and Langford, 2002). According to the structure of *Nicotiana tabacum* myosin XI, they can be roughly divided into four domains (Tominaga et al., 2003), which is similar to its homologue in animal cells, myosin V. They contain an N-terminus motor domain, neck domain, which contains six IQ motifs, a rod region, which contains an α-helical coiled-coil structure, and a tail domain at the C terminus. Using an actin sliding assay, Tominaga found the maximum velocity of myosin XI from tobacco BY-2 cells is 7 μm s^{-1} (Tominaga et al., 2003), which is about 10 times faster than myosin Va (Mehta et al., 1999). The fastest motor protein currently known is a myosin XI from the alga *Chara corallina*, which can reach 50-70 μm s^{-1} (Ito et al., 2007). Tominaga *et al.* showed that, similar to myosin V, myosin XI is a plus-end directed actin dependent motor with a step size of 35 nm (Tominaga et al., 2003).

Similarly to its homologue myosin V, myosin XI is responsible for organelle and vesicle transport (Reisen and Hanson, 2007; Peremyslov et al., 2008; Sparkes et al., 2008; Peremyslov et al., 2012). It also has been shown to be critical for cell polarity and tip growth, as knocking down myosin XI in *P. patens* causes a severe growth defects (Vidali et al., 2010; Furt et al., 2013).

Given the fact that both tip growth and cytokinesis in plants need vesicle trafficking and exocytosis (Reichardt et al., 2007; Rybak et al., 2014), myosin XI might play a role in plant cell division. So it is reasonable to investigate the function of myosin XI during cell division.

1.4.2 Vesicles

Golgi-derived vesicles are critical for the formation of the cell plate (Segui-Simarro et al., 2004). Different vesicle markers can be used to study the localization and dynamics of these vesicles. Two types of vesicle markers, vesicle associated membrane proteins (VAMPs) and Rab-GTPases, are discussed below because they were selected for the present work.

Vesicle associated membrane proteins, also known as VAMPs, are a family of SNARE proteins, which share similar structures and function in vesicle fusion. In *Arabidopsis thealiana*, it was found that double knockout of VAMP721 and VAMP722 is lethal (Lipka et al., 2007; Kwon et al., 2008); mutations of both VAMP721 and VAMP722 also cause defects in cell plate formation (Zhang et al., 2011). When the localization of VAMP721 and VAMP722 was investigated, there was almost no signal in the cytoplasm, while there was a clear accumulation of both proteins at the cell plate (El Kasmi et al., 2013). Together, these results support the participation of this protein in cell plate formation. However, to this date, no information is available about the localization of VAMPs in *P. patens* during cell division.

A different type of marker that can be used to track vesicle behavior is the Rab-GTPases. Rab-GTPases are a superfamily of small GTPases that regulate intracellular vesicle transport. In *A. thaliana*, Qi et al. showed that one subfamily of Rab-GTPases, RabAs, but not RabDs, are important for vesicle trafficking in the trans-Golgi network (Qi and Zheng, 2011). Because the formation of the cell plate requires these Golgi-derived vesicles, it is expected that RabAs participate in plant cytokinesis. Indeed, Chow et al. have shown that RabAs are important for cytokinesis and they showed RabAs accumulate at the cell plate (Chow et al., 2008). In *P. patens*, we know there are three types of RabAs (Agar), but their localization during cytokinesis has not been investigated.

1.4.3 Endoplasmic Reticulum

The endoplasmic reticulum (ER) has many important functions, including protein folding and protein transport. Related to these functions, during interphase in plant cells, ER typically has three types of formations: the polygonal cortical ER arrays, the nuclear surrounding ER, and the ER that connects the other two types (Boevink et al., 1998; Ridge et al., 1999; Nebenfuhr et al., 2000; Gupton et al., 2006).

Beside these localizations during interphase, the ER also has a specific localization during cell division. In tobacco NT-1 cells, before the nuclear envelope breaks down, the ER starts invading the nuclear envelope when the chromosomes begin to condense (Gupton et al., 2006). During metaphase and anaphase, the ER becomes tubules lining up with microtubules in the mitotic spindle (Gupton et al., 2006). Finally, during cytokinesis, the ER also appears at the phragmoplast, where it is assumed that it delivers components to support the development of the cell plate (Gupton et al., 2006). No information is available about the localization of the ER during cell division in *P. patens*. But we know that in other plants, myosin XI attaches to the ER membrane and plays a role in controlling the dynamics and localizations of the ER (Yokota et al., 2009; Yokota et al., 2011). Thus it is also important to investigate the colocalization of myosin XI and the ER during *P. patens* cell division.

1.5: Hypotheses and Objectives

As summarized by Gerd, plant cytokinesis is a process of “fission by fusion” (Jurgens, 2005a); numerous vesicles are required in the division plane to build the cell plate. Thus vesicle transport is an important process during plant cell division. Based on the importance of myosin XI in polarized transport (Reisen and Hanson, 2007; Peremyslov et al., 2008; Sparkes et al.,

2008; Vidali et al., 2010; Peremyslov et al., 2012), my hypothesis is that myosin XI may play a role in plant cell division.

My goal for this project is to determine the possible role of myosin XI in plant cell division. These are the objectives I propose to achieve:

1. Determine the localization of myosin XI during cell division.
2. Determine the localizations of F-actin, Golgi-derived vesicles and the endoplasmic reticulum in relation to myosin XI.
3. Use specific inhibitors to determine how they affect the localization of myosin XI during cell division.

2. MATERIAL AND METHODS

2.1. Plant Material

2.1.1 Cell Lines Used

All cell lines used in this study were derived from the moss *Physcomitrella patens* (Hedw.) Brunch & Schimp. Gransden strain, and most of them were made in Vidali lab (LV lines). For microtubule imaging, tubulin EGFP line (GTU14) (Hiwatashi et al., 2008) was used. For GFP control imaging, 3mEGFP line (LV754) was used. For myosin XI imaging, both Myosin XIa-3mEGFP and 3mCherry-RabA53 line, and Myosin XIa-3mEGFP and ER-mCherry line (constructed by me, LV832) were used. For actin imaging, LA2W-myo BKO line (LV765) was used. For VAMP imaging, 3mEGFP-Myosin XIa and 3mCherry-VAMP line (LV653) was used. For RabAs and myosin XI colocalization imaging, Myosin Xia-3mEGFP and 3mCherry-RabA53 line, and 3mCherry-RabA53 and 3mEGFP-RabA21 line were used. For endoplasmic reticulum and myosin XI colocalization imaging, Myosin XIa-3mEGFP and ER-mCherry line (LV832) was used.

2.1.2 Cell Line Passing

One half plate of one week old *P. patens* was collected and placed into a 14 ml culture tube with 2 ml sterile water. The tissue was ground with a grinder (Fisher Power Gen 125), at top speed (30,000RPM) for 20 seconds. The ground tissue was spread into cellophane covered solid media plates (700 µl tissue per plate). For routine cell line expansions, PpNO3 plates were used, and for transformation, PpNH4 plates were used; all the plants were grown at 25 °C in a growth chamber.

2.1.3 Construct Preparation

The mCherry fragment was amplified by PCR from plasmid: pTHUbigate-lifeact-mCherry. The forward primer was WPI 278 (attB5-mCherry-mEGFP. Sequence: GGGGACAACTTTGTA

TACAAAAGTTGTGATGGTGAGCAAGGGCGAGGAG) and the reverse primer was UM 481 (attB2_GFP_KDEL. Sequence: GGGGACCACTTTGTACAAGAAAGCTGGGTATCATAGCT

CATCTTT CTTGTACAGCTCGTCCAT). The PCR product was ligated into pDONR P5P2 plasmid by BP reaction. The construct was then put into pTHUbigate plasmid by LR reaction with empty pTHUbigate plasmid, PENT P1P5r plasmid and the BP reaction product.

2.1.4 Stable Transformation

Nine ml of 8% mannitol and 3 ml of driselase (Sigma D9515-25G, 0.5% final concentration) were mixed in a sterile Petri dish. Six day old moss tissue was harvested from PpNH4 plates and transferred to the driselase solution. The dish was placed on the ROTO-SHAKE, shaken at speed 2 at room temperature for 1 hr. Protoplasts were harvested by filtering the digestion product through a sterile filter (Cell strainer 70 μm Nylon). The protoplast solution was centrifuged at 700 rpm (250 g) in IEC CENTRA-7 centrifuge for 5 min. The supernatant was discarded, and the pellet was resuspended gently with 10 ml of 8% mannitol. The protoplasts were centrifuged and resuspended with 8% mannitol twice to wash out driselase. Cell number was counted with a hemocytometer after the wash step. Then, the protoplasts were resuspended with MMg medium to be at a final concentration of 1.6 x 10^6 protoplasts/ml of MMg. The protoplasts were left at room temperature for 20 min. 600 μl of protoplasts were mixed gently with 60 μg of linearized construct. 700 μl of PEG 4000/Ca was then added. The mixture was left at room temperature for 30 min, then diluted with 3 ml of W5 medium. The diluted protoplasts were centrifuged at 700 rpm (250 g) for 5 min to remove PEG. The

supernatant was discarded and the pellet was resuspended with 2 ml of melted PRMT/$CaCl_2$. The protoplast solution was spread into 2 cellophane-covered PRMB plates (1 ml/plate). The plates were sealed with micropore tape and placed in a 25°C growth chamber. Four days after the transformation, the cellophane, along with the transformed plants, was transferred to selective medium plate. One week later, the cellophane was transferred to a normal PpNH4 plate. One week after that, the cellophane was transferred back to a selective medium plate. One week later, the surviving plants were picked and placed in a new selective medium plate. When the plants were big enough, they were expanded to one PpNH4 plate (to maintain the line) and one PpNO3 plate (to screen the line by confocal microscopy).

2.1.5 Preparation of Moss Samples For Imaging

MatTek 35mm Glass Bottom Dishes (holey slides) were sterilized by exposing them to UV light for 20 minutes. A sterile 1000 µl sterile pipet tip was placed upside down on the bottom of the plate in the middle of the glass. Solid PpNO3 media was melted in the microwave oven. 5 ml was added to the plate around the tip and left to solidify for 20 minutes. After the tip was removed, 70 µl of melted solid PpNO3 media was added in the plate inside the hole and spread well with a sterile pipet tip. A small piece of moss tissue from a one week old PpNO3 plate was placed horizontally inside the hole. The plates were taped with micropore tape (3M Micropore™) and placed in the growth chamber. Cells were observed at least 4 days after plating.

2.2. Imaging and Data Analysis

2.2.1 Imaging

For all imaging, the inverted Nikon Ti microscope was used with a 60X lens (Nikon Apo TIRF, NA=1.49). When imaging, the chamber with 1-2 week old plants was placed on the stage. Z-stacks at 0.5 μm intervals, with 7-9 planes, were acquired for multiple colors for each cell. Multiple cells were imaged with a 2 minute interval; with this setup, a total of 3-5 cells can be simultaneously recorded. The exposure time was 50 msec, and the intensity of the LED illuminator was adjusted, depending on the sample.

For samples without drug treatment and with latrunculin B (LatB) treatment, the lengths of the movies were 6-8 hours, and for samples with BFA treatment, the length of the movies were less than 3 hours. For the low concentration of LatB treatment, 200 μl of 10 μM LatB were added into the hole of the chamber. For high concentration of LatB treatment, a total of 500 μl of 100 μM LatB were added to the dish. 200 μl were placed in the hole and 300 μl were spread on the gel around the hole. When treated with brefeldin A (BFA), 200 μl of 10 μM BFA was added into the dish. Imaging acquisition started 20 minutes after adding the drug.

2.2.2 Data Analysis

As shown in **Figure II.1**, for data analysis, frames that contain cell division events were duplicated from raw images. Then the duplicated images were rotated to make sure every cell was in the same orientation. A 250 pixels X 250 pixels area was cropped around where cell division happened. In the movies presented, the last frame where the nuclear envelope was still intact was set as frame 1 and time 0. Multiple Z planes will be projected into single plane image.

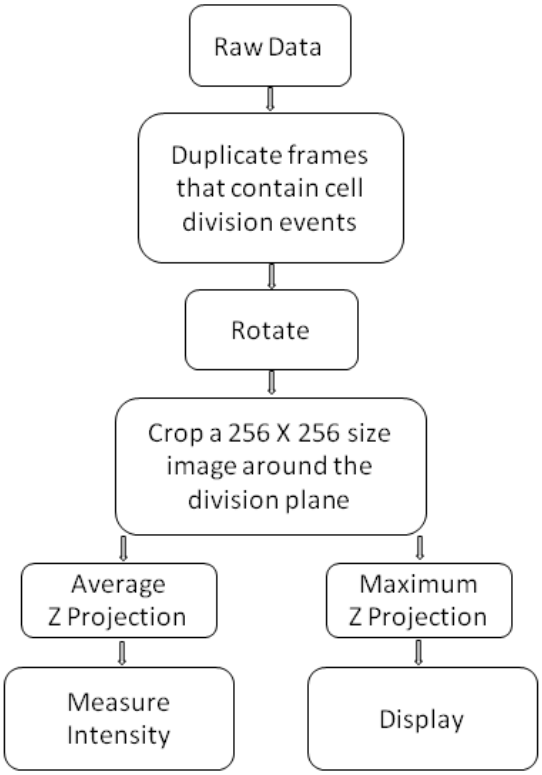

Figure II.1. Flow chart of data processing.

To measure the signal intensity changes on the spindle and at the phragmoplast, all the multiple planes movies were Z-projected by average intensity. A rectangular shaped region of interest was made bordering the division plane and the mean of signals in that area (**Ms**) was measured over time by ImageJ. The length and width varied a little, depending on the width of the cell, but the ratio of length to width was kept constant at 5:3 to make sure the similar portion of the cell was measured. The background signal (**Mb**) was measured by measuring the mean of the signal in some place outside and away from the cells.

After obtaining these values, the background was subtracted from Ms. But because different cells had different expression levels of labeled proteins, and the positions of the cells in

the dish also affected the illuminations, after the background was subtracted, there still were differences between different cells in fluorescence intensity. To make the signals more comparable they were normalized by the signal immediately after nuclear envelope breakdown: (Ms-Mb) in each frame was divided by (Ms-Mb) in the second frame to get the relative fluorescent intensity of the signals (Mr) at the division plane.

$$\mathbf{Mr_i = (Ms_i - Mb_i)/(Ms_2 - Mb_2)}$$

Mr shows the fluorescent changes relative to the initial fluorescent intensity after the nuclear envelope breaks down. The second frame was used to correct this because when the nuclear envelope is still intact, there is a fluorescence void in the region of interest, thus it cannot show the differences that are useful for comparison. The second frame could always show the initial fluorescence quite well, though there was always a small accumulation of myosin XI in the second frame, which reduced slightly the relative accumulation of myosin XI.

3. RESULTS

3.1. Timing for Cell Division

To test whether I could record *Physcomitrella patens* cell division efficiently with fluorescence microscopy, I used a moss line expressing α-tubulin tagged with sGFP (Hiwatashi et al., 2008). I found that after nuclear envelope breakdown, the mitotic spindle appeared in the next frame (**Figure 1**). At approximately 12 min after nuclear envelope breakdown, the phragmoplast formed and started expending towards the periphery. Phragmoplast formation is evident by the change in the configuration of the microtubule array from elongated spindle to box-like (**Figure 1, 12 min panel**). Based on this result, I used 12 min as the timing for the formation of the phragmoplast.

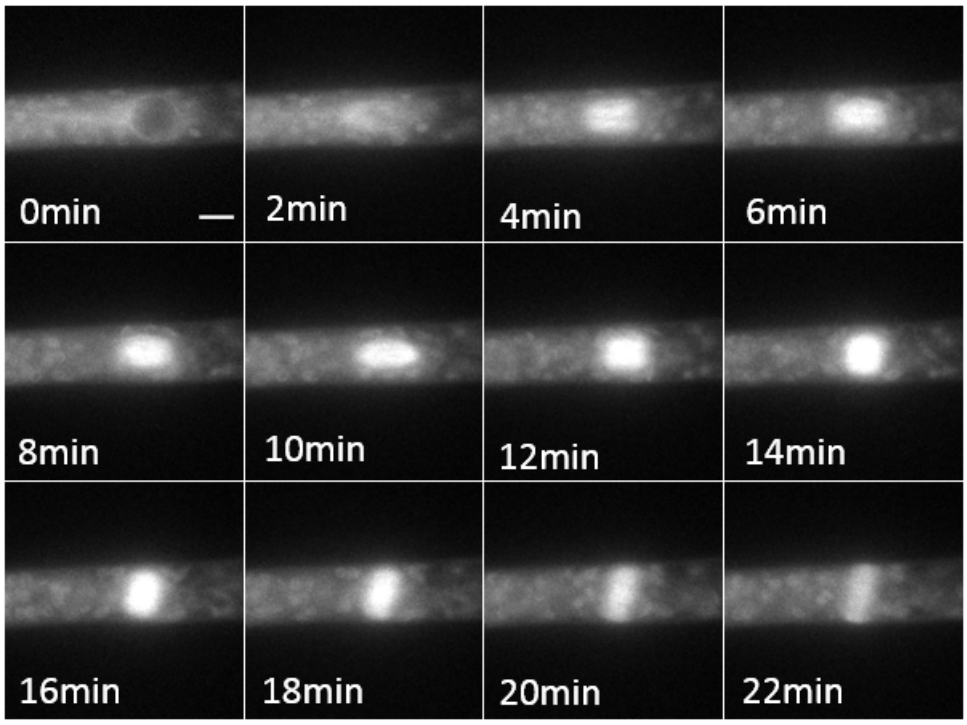

Figure 1. Example of cell division in tubulin-sGFP line. After the nuclear envelope breaks down at time 0, the spindle forms at the division plane. Typically, 12 min later, the phragmoplast forms in the middle of the division plane and starts to expand towards the side membrane of the dividing cell. (Scale bar: 10 um)

3.2. Myosin XI and Actin Localization

To examine the localization of myosin XI during cell division, I used two moss lines derived from a line in which myosin XIa had been tagged at its C terminus with three copies of mEGFP (myosin XI-3mEGFP). The behavior of myosin XI-3mEGFP in both lines seemed identical.An example of this behavior is shown in **Figure 2A**. In both lines, myosin XI started accumulating on the spindle, immediately after nuclear envelope breakdown. After approximately 12 min, the localization of myosin XI changed into a fine line along the center of the phragmoplast. As shown in **Figure 2B**, the quantification of the accumulations of myosin XI in both lines showed that they are very similar to each other and wer clearly different from that of 3mEGFP alone (Compare **Figure 2 and 3**). The clear difference between the localization of myosin XI-3mEGFP and 3mEGFP indicates that myosin XI accumulates specifically on the mitotic spindle and the phragmoplast.

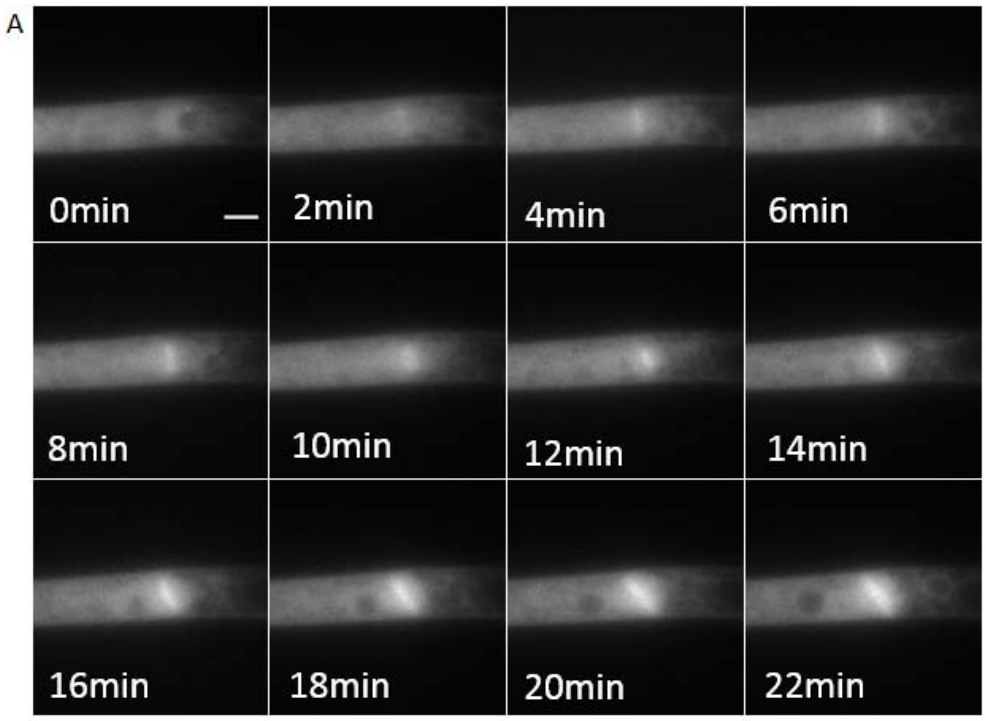

Figure 2 continued

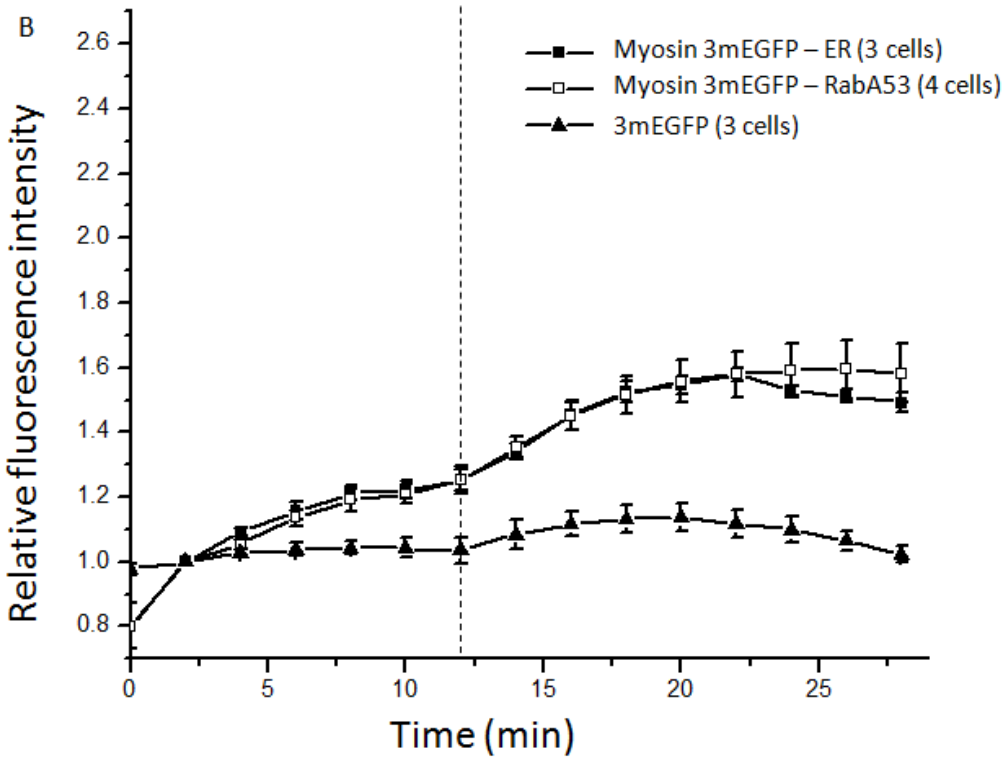

Figure 2. Myosin XI localization during cell division. **A**. A representative example of the localization of myosin XI during cell division. After nuclear envelope breaks down at time 0, myosin XI accumulates in the middle of the spindle and after the formation of the phragmoplast, myosin XI forms a fine line along the cell plate at the phragmoplast. (Scale bar: 10 μm) **B**. The relative fluorescence intensity of myosin XI at the division plane during cell division. The dash line is at time 12, when the formation of the phragmoplast begins. Error bar shows standard error of the mean.

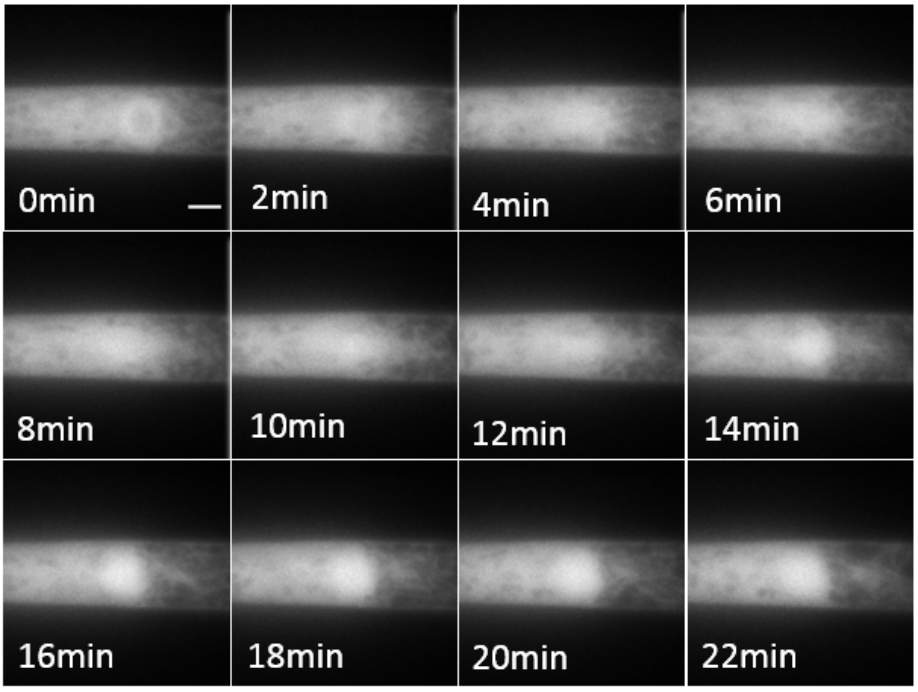

Figure 3. **Example of cell division in 3mEGFP control line**. After the nuclear envelope breaks down, there is no clear accumulation of EGFP signal at the division plane. Because there is more accessible volume at the phragmoplast, more diffusing mEGFP signal appears at the division plane. (Scale bar: 10 μm)

To determine if the localization of myosin XI coincided with that of filamentous actin, I observed the localization of actin filaments during cell division using the lifeact-mEGFP line. Surprisingly, I found that actin did not accumulate on the mitotic spindle, in contrast to myosin XI, but did localize later at the phragmoplast (**Figure 4A**). Quantification of the increase of F-actin signal was above background levels as determined by comparing with the level of diffusing 3mEGFP. These results suggest that in *P. patens* protonemata, F-actin is not present on the mitotic spindle, but it accumulates at the phragmoplast.

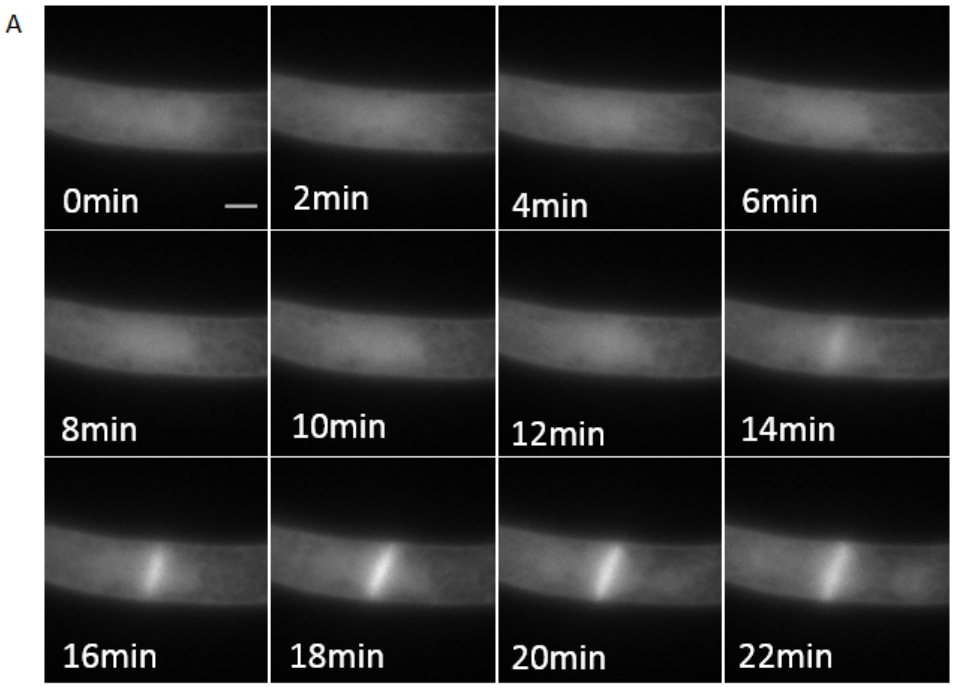

Figure 4 continued

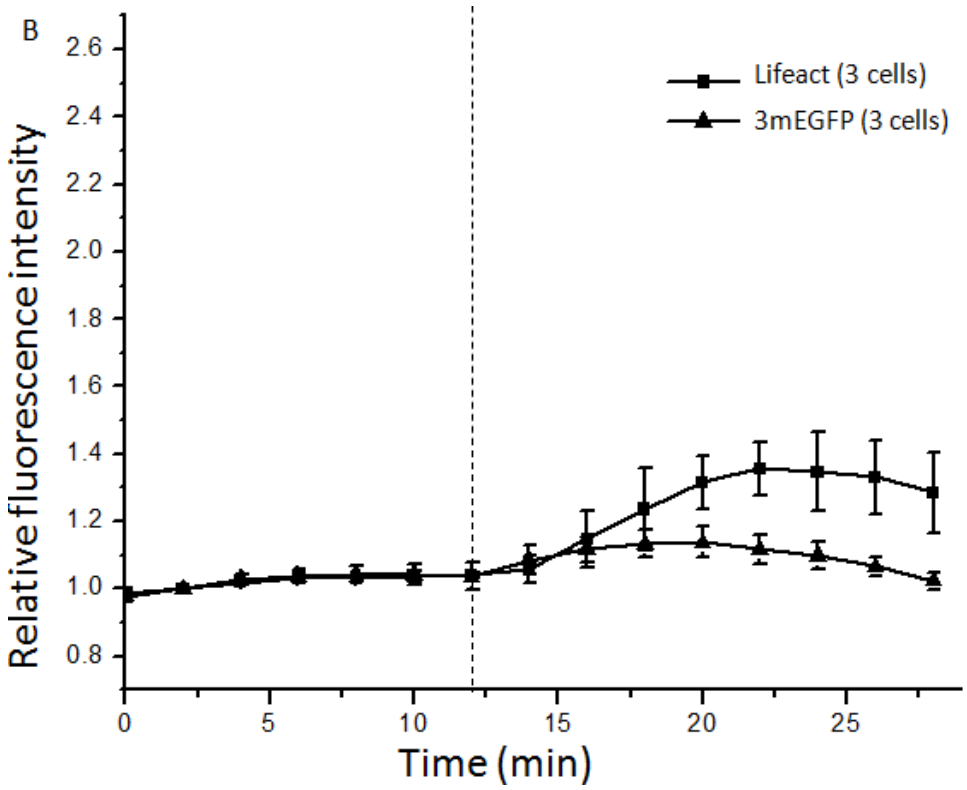

Figure 4. F-actin localization during cell division. A. A representative example of the localization of F-actin during cell division. After nuclear envelope breaks down at time 0, there is no accumulation of F-actin on the spindle, but after the formation of the phragmoplast at time 12 min, actin filaments start to accumulate along the cell plate at the phragmoplast. F-actin was visualized with lifeact-mEGFP (Scale bar: 10 μm) **B**. The relative fluorescence intensity of actin at the division plane during cell division. The dash line is at time 12, when the formation of the phragmoplast begins. Error bar shows standard error of the mean.

To test the effect of depolymerizing F-actin on the localization of myosin XI, I used the actin depolymerization drug, latrunculin B (LatB). Initially, I used 200 µl of 10µM LatB to depolymerize actin. After I added the drug, the tip cells stopped growing quickly and the actin accumulation at the phragmoplast was inhibited (**Figure 5**); however, cell division was not inhibited. I found that myosin XI still accumulated on the spindle and at the phragmoplast, though it seemed that LatB had some effects on the accumulation of myosin XI at the phragmoplast (**Figure 6 and 7B**). To verify that I depolymerized all the actin filaments in the cell, I used a higher concentration of LatB (100 µM) (Figure 5B and 6B). Despite the higher concentration of LatB, I was still able to find dividing cells, and the results were very similar to those from the 10 µM LatB treatment (**Figure 6**). Using one–way ANOVA, I analyzed fluorescence intensities from times 8 and 22 min (**Figure 7C and 7D**), and found that at time 8 min, myosin XI accumulation, with and without LatB treatment, was significantly different from the 3mEGFP group, while at time 22 min, each group was significantly different from others (**Figure 7D**). These results suggest that two different mechanisms exist for myosin XI accumulation: an F-actin independent mechanism at the spindle and partially at the phragmoplast, and an F-actin dependent one for the rest of myosin XI at the phragmoplast.

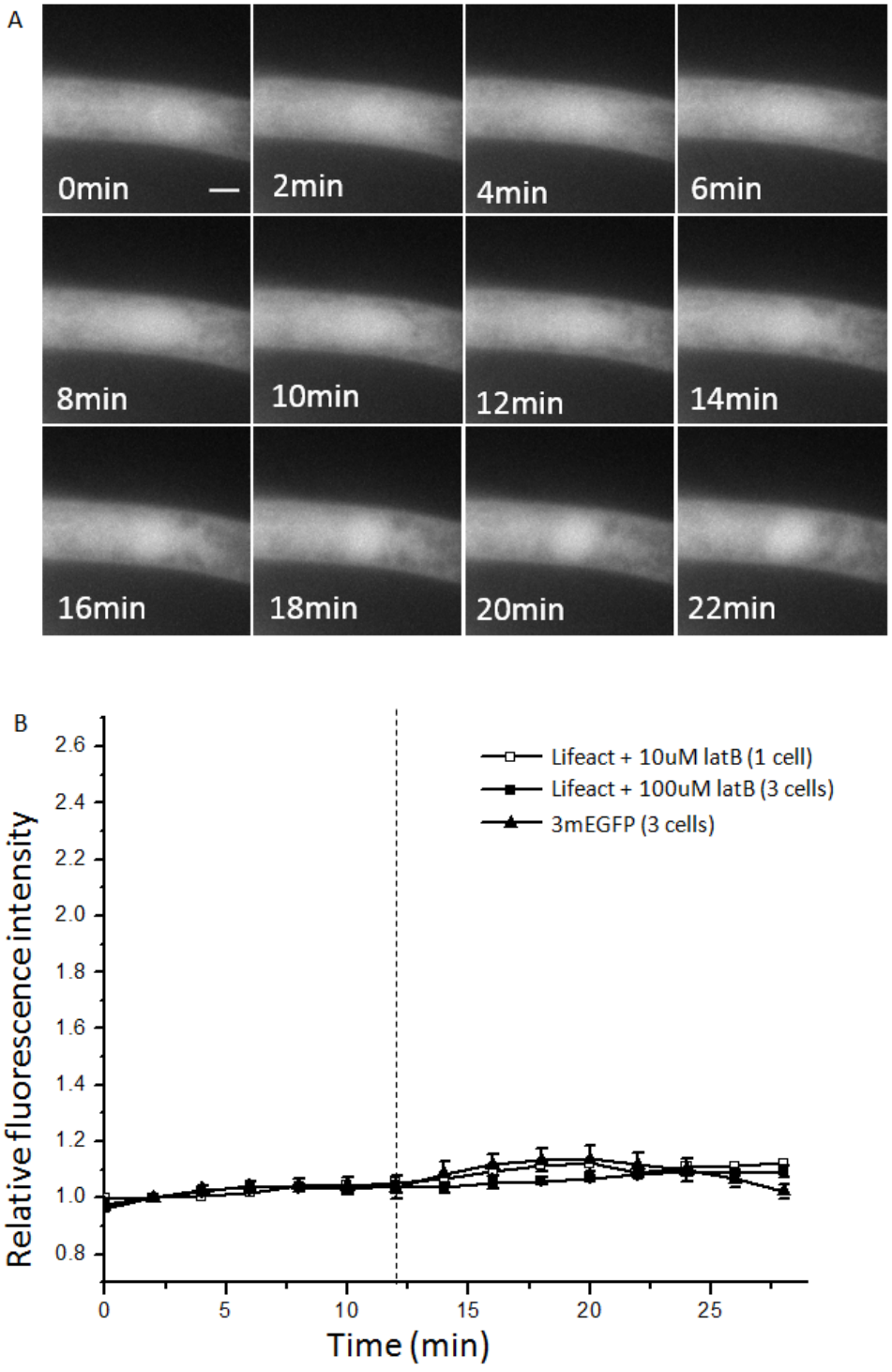

Figure 5. F-actin localization after 10 µM-100 µM Latrunculin B treatment. A. A representative example of the localization of F-actin during cell division following LatB treatment. No clear accumulation of F-actin anywhere during the cell division is observed, similar to the localization of diffusing EGFP. (Scale bar: 10 µm) **B**. Quantification of the relative fluorescence intensity of lifeact-mEGFP labeled F-actin at the division plane during cell division with LatB. The dash line is at time 12, when the formation of the phragmoplast begins. Error bar shows standard error of the mean.

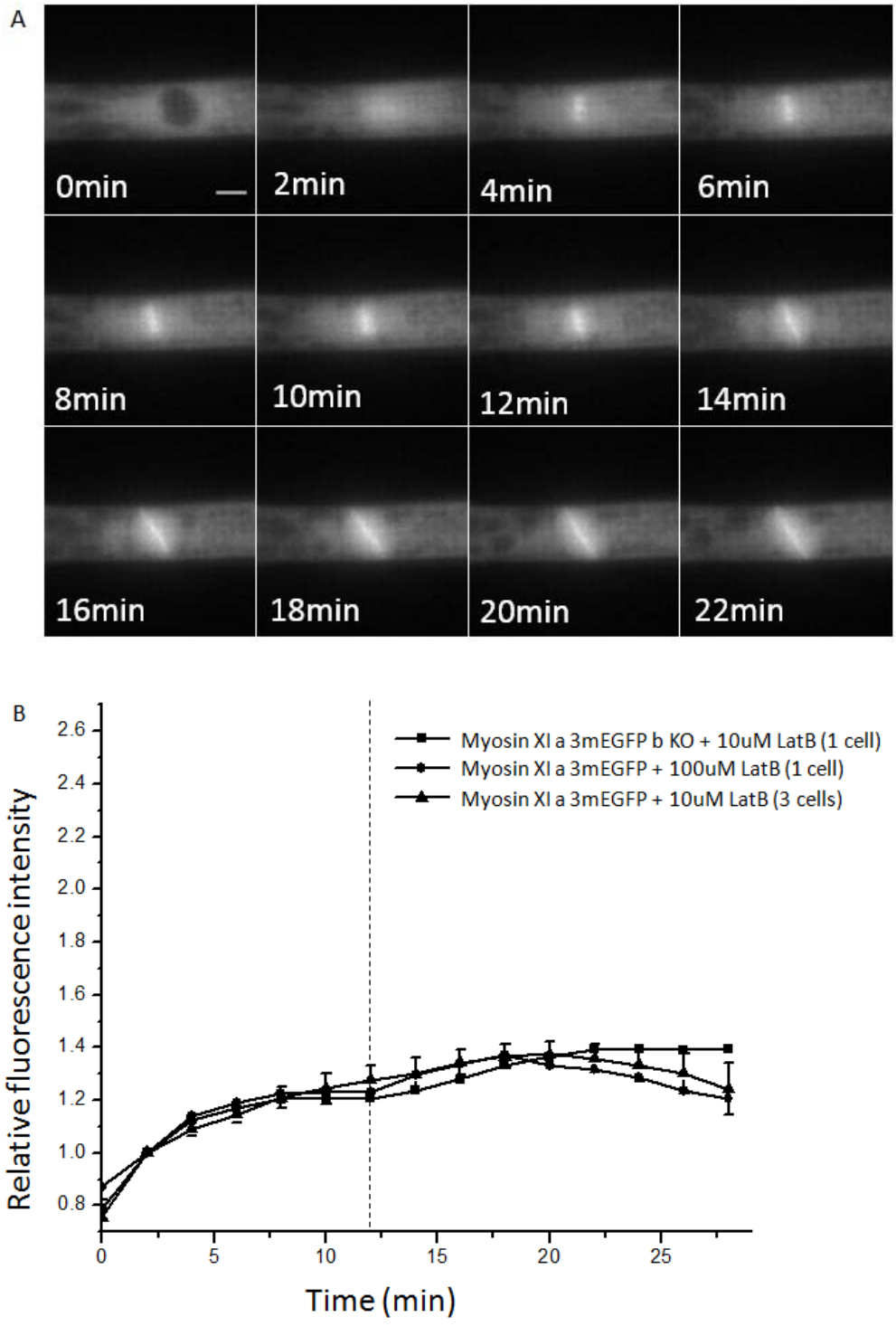

Figure 6. Myosin XI localization with 10 µM-100 µM LatB treatment. A. A representative example of the localization of myosin XI during cell division following LatB treatment. Myosin XI still accumulates at both the spindle and the phragmoplast after depolymerizing actin filaments with LatB (Scale bar: 10 µm) **B**. Quantification of the relative fluorescence intensity of myosin XI-3mEGFP at the division plane during cell division in the presence of LatB. Error bar shows standard error of the mean.

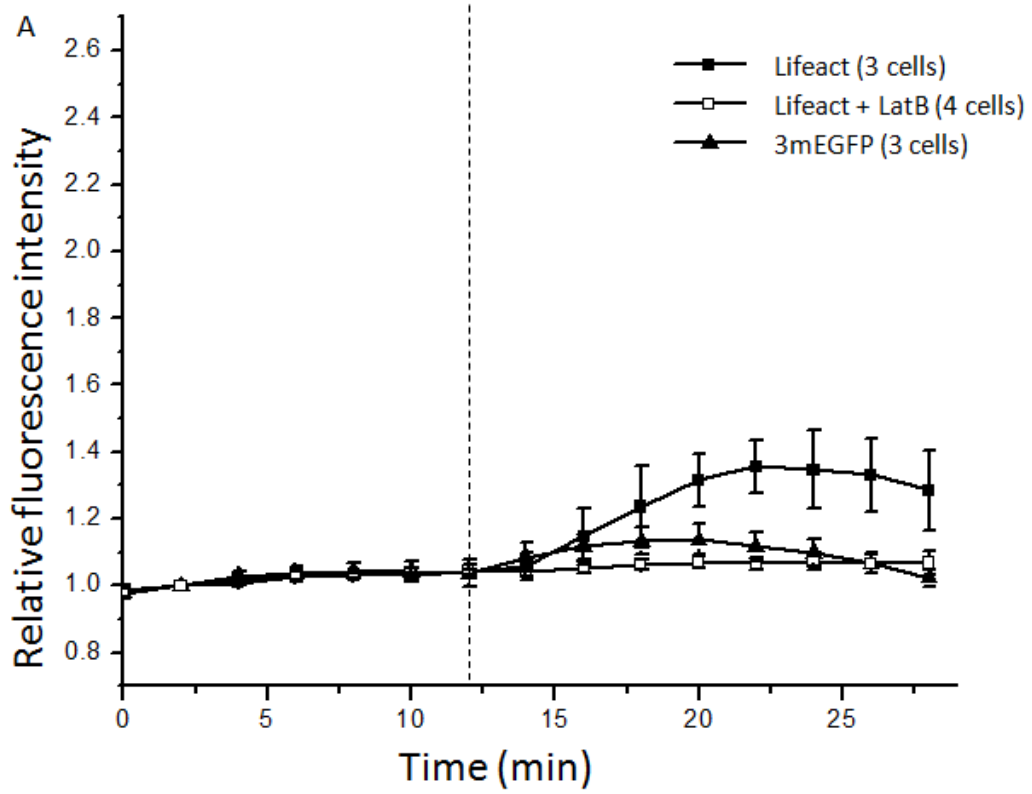
A
Relative fluorescence intensity
Time (min)
Lifeact (3 cells)
Lifeact + LatB (4 cells)
3mEGFP (3 cells)

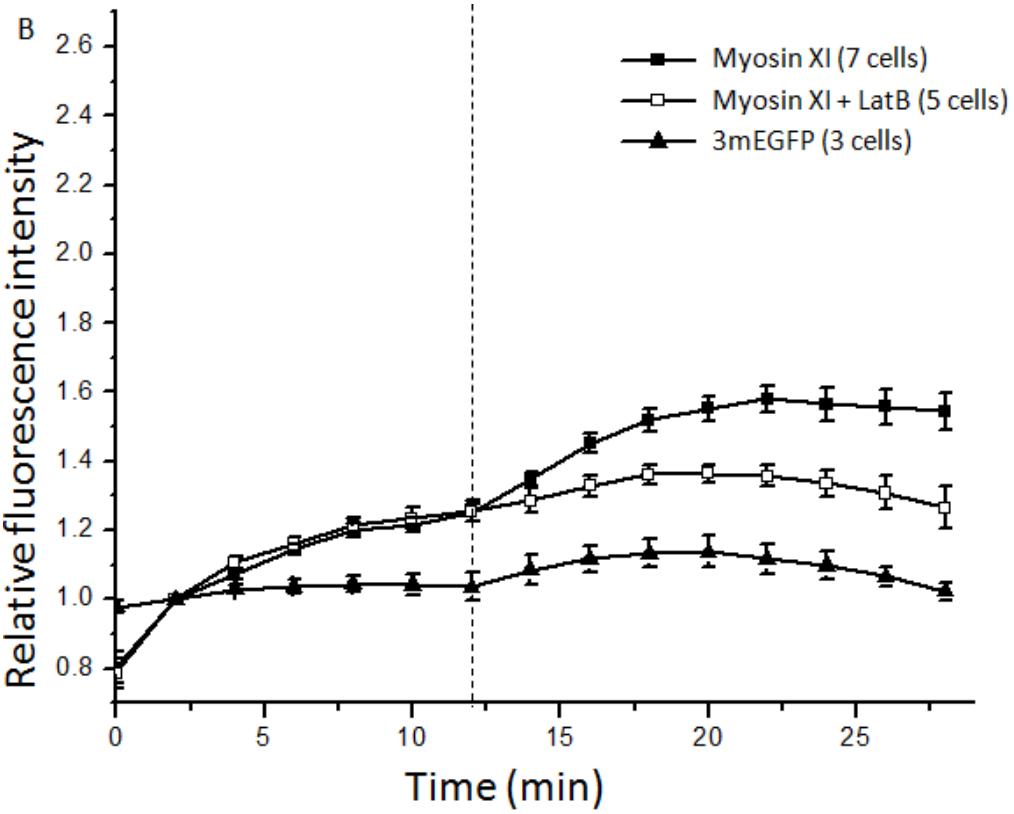
B
Relative fluorescence intensity
Time (min)
Myosin XI (7 cells)
Myosin XI + LatB (5 cells)
3mEGFP (3 cells)

Figure 7 continued

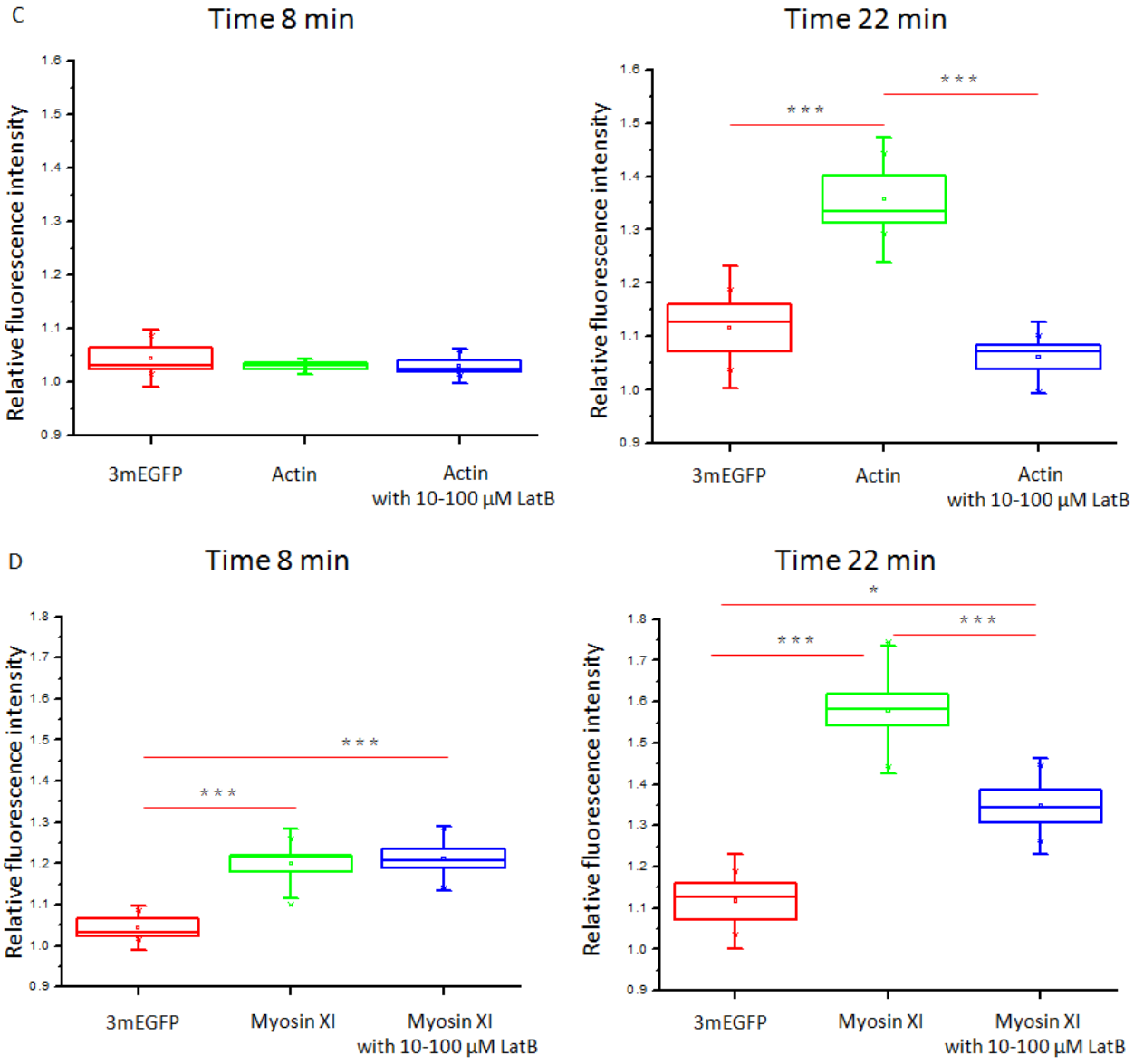

Figure 7. Comparison of F-actin and myosin XI signals during cell division with different Latrunculin B treatments. A. The relative fluorescence intensity of actin at the division plane during cell division with or without LatB. In the absence of LatB, F-actin accumulates only at the phragmoplast, but when in presence of LatB, no matter in which condition, the lifeact-mEGFP signal becomes similar to the signal of 3mEGFP. **B**. The relative fluorescence intensity of myosin XI-3mEGFP at the division plane during cell division with or without LatB. The accumulation of myosin XI on the spindle is not affected by depolymerizing F-actin, but the accumulation of myosin XI at the phragmoplast is partially inhibited by LatB treatment. In both A and B, the dash line is at time 12, when the formation of the phragmoplast begins. Error bar shows standard error of the mean. **C** and **D** show the statistical analysis in chosen time points, 8 min and 22 min from Figure 7 A and B, respectively. Box represents standard error of the mean and the whisker represents standard deviation. ＊means P<0.05, ＊＊＊Means P<0.01.

3.3. Myosin XI and Vesicles

To further investigate the actin-independent localization of myosin XI, I tested the possibility that myosin XI was being brought to these locations passively by vesicles. To visualize vesicles, I used two types of vesicle marker: the v-SNARE--vesicle associated membrane proteins (VAMPs), and members of vesicle trafficking regulatory proteins--RabAs. All the vesicle markers that I tested accumulated only at the phragmoplast, but not at the mitotic spindle (**Figure 8, 9 and 10**). Hence, these vesicles are likely bringing materials to the cell plate, but not the spindle. When comparing the level of accumulation of different RabAs, I found there was a significant difference between RabA53 and RabA21 (**Figure 10C**), thus it seems *P, patens* protonemata cells were using these vesicles selectively. Interestingly, when I treated the 3mCherry-VAMP line with LatB, I also observed a decrease of VAMP signal at the phragmoplast, similar to the case of myosin XI (**Figure 11**). Together, these results indicate that the VAMP and RabA-labeled vesicles are not responsible for the actin-independent localization of myosin XI to the mitotic spindle.

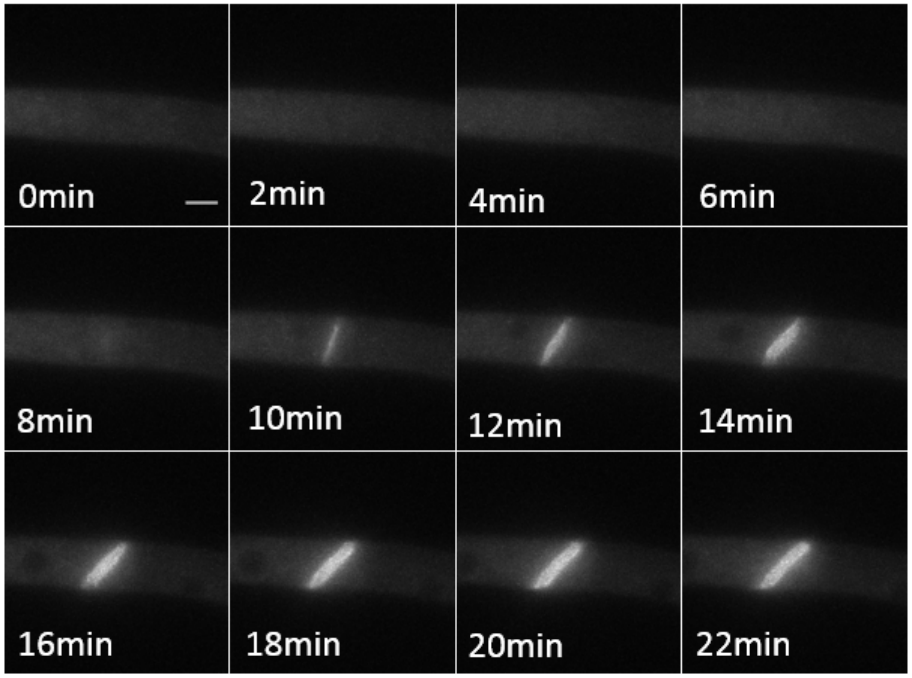

Figure 8. Localization of 3mCherry-VAMP during cell division. A representative example of the localization of 3mCherry-VAMP labeled vesicles during cell division. Note that there is no accumulation of VAMP signal on the spindle but VAMP signal increases significantly at the division plane after the phragmoplast is formed. (Scale bar: 10 μm)

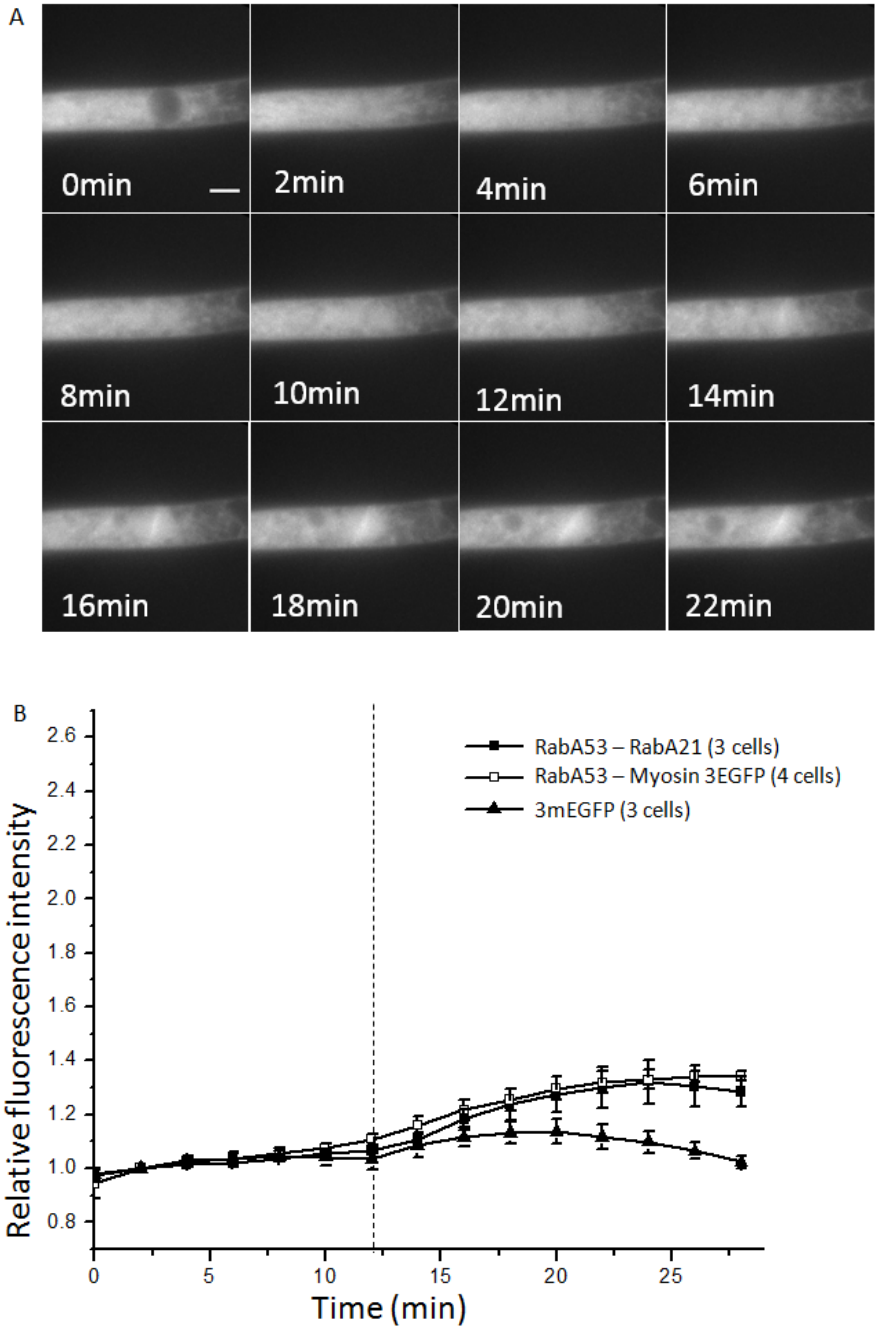

Figure 9. RabA53 localization during cell division. A. A represenative example of the localization of 3mCherry-RabA53 during cell division. There is no accumulation of RabA53 on the spindle (2-10 min), but after the formation of the phragmoplast at 12 min, there is a weak accumulation of RabA53 along the cell plate. (Scale bar: 10 µm) **B**. The relative fluorescence intensity of RabA53 at the division plane during cell division. In both RabA53 lines, the accumulation of RabA53 signal is only visible at the phragmoplast, and the accumulation pattern is almost identical. The dash line is at time 12, when the formation of the phragmoplast begins. Error bar shows standard error of the mean.

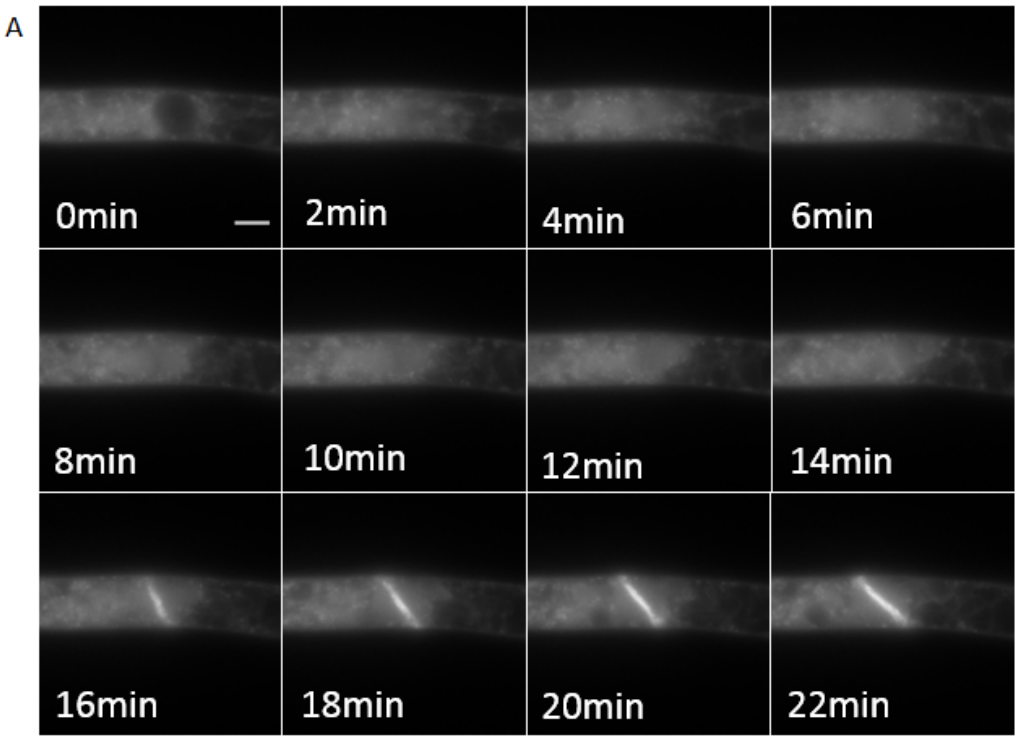
A
0min
2min
4min
6min
8min
10min
12min
14min
16min
18min
20min
22min

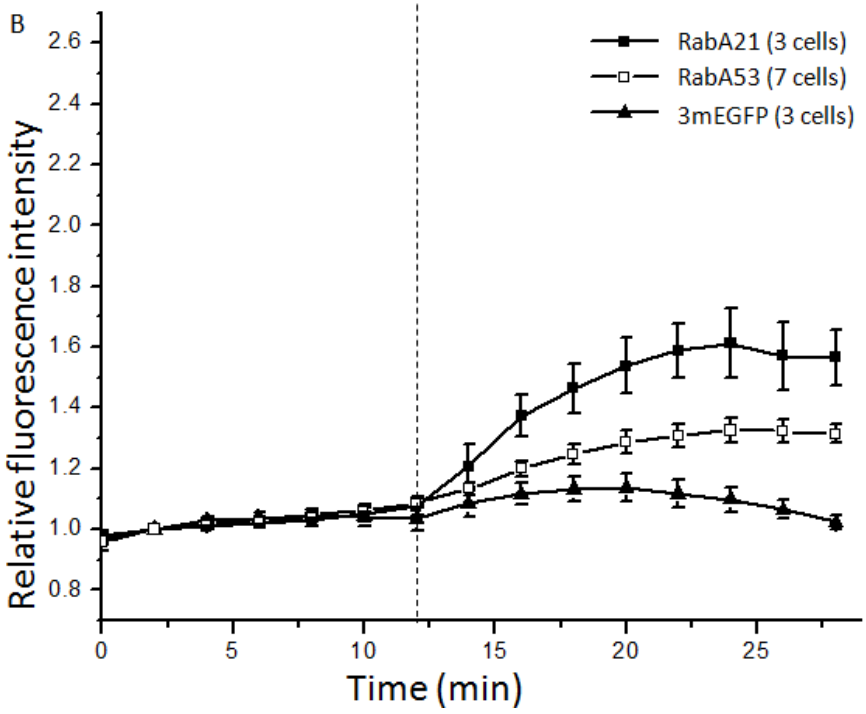
B
RabA21 (3 cells)
RabA53 (7 cells)
3mEGFP (3 cells)
Relative fluorescence intensity
Time (min)
0.8
1.0
1.2
1.4
1.6
1.8
2.0
2.2
2.4
2.6
0
5
10
15
20
25

Figure 10 continued

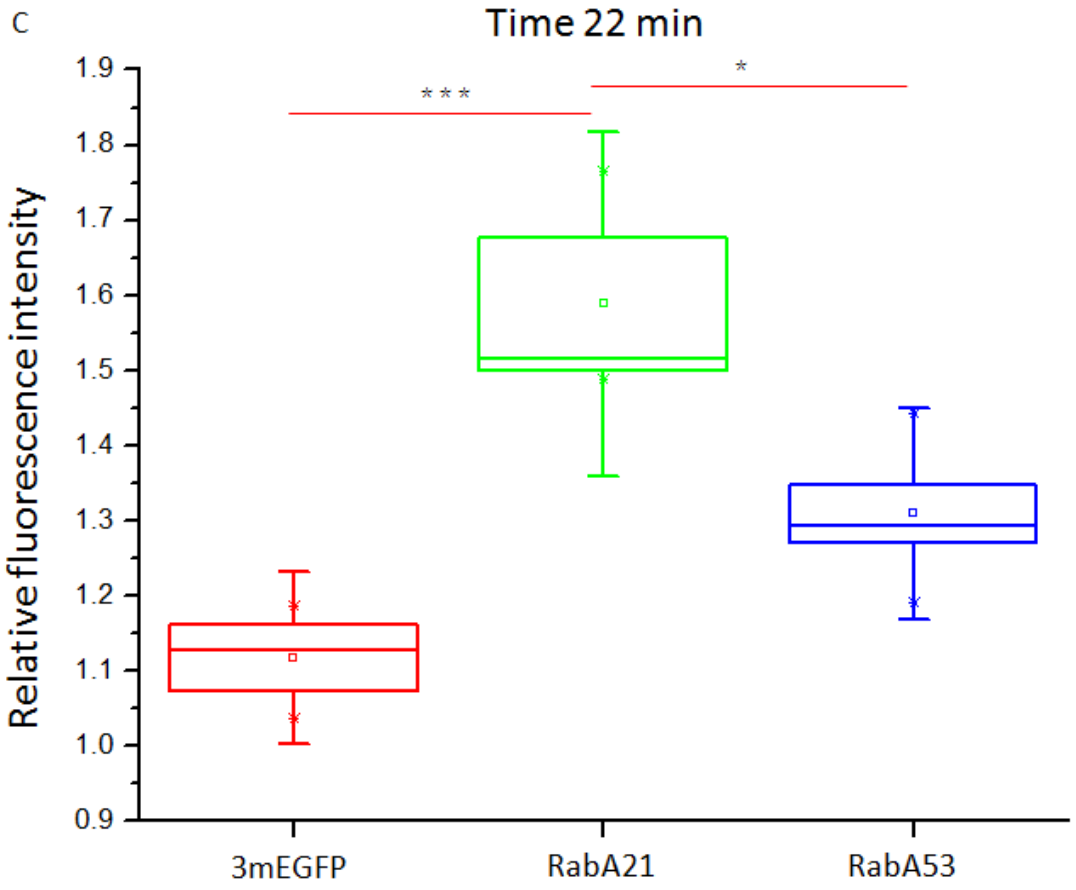

Figure 10. RabA21 localization during cell division. A. A representative example of the localization of 3mEGFP-RabA21 during cell division. There is no accumulation of RabA21 on the spindle, but it accumulates along the cell plate after the formation of the phragmoplast. (Scale bar: 10 µm) **B.** The relative fluorescence intensity of RabA21 at the division plane during cell division. Similarly to RabA53 signal, before the formation of the phragmoplast, they are identical to 3mEGFP signals, but after the formation of the phragmoplast, the behaviors of these markers are different from diffusing 3mEGFP. The dash line is at time 12, when the formation of the phragmoplast begins. Error bar shows standard error of the mean. **C.** shows the statistical analysis in chosen time points, 22 min from Figure 10 B. Box represents standard error of the mean and the whisker represents standard deviation. ＊means P<0.05, ＊＊＊Means P<0.01.

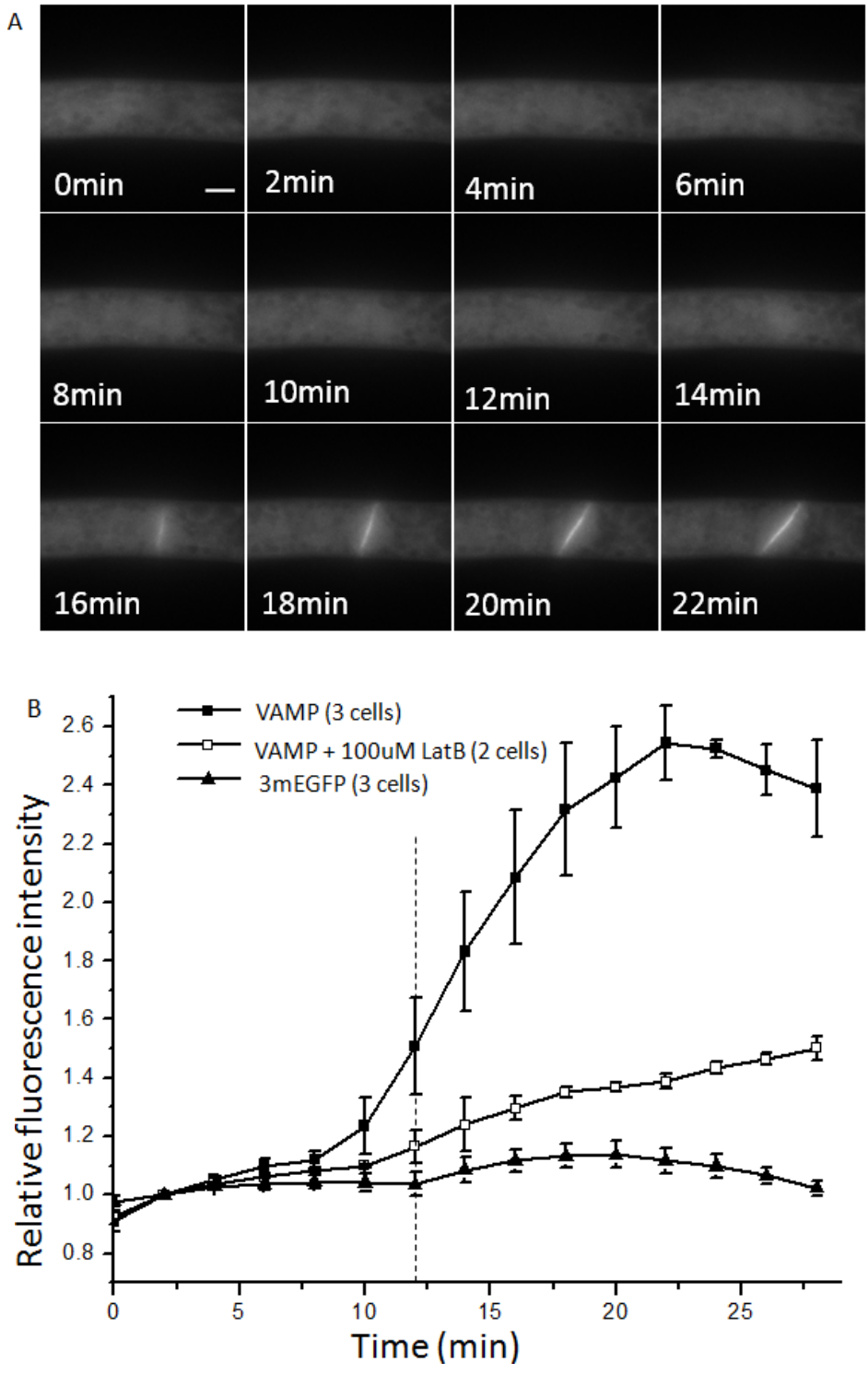

Figure 11. Legend in the next page.

Figure 11. VAMP localization in the absence of F-actin. A. A representative example of the localization of VAMP during division of a cell treated with 100 μM LatB. Compared with Figure 8, the behavior of VAMP in the presence and absence of LatB treatment seems similar, but the accumulation of VAMP at the phragmoplast seems weaker when cells are treated with LatB. (Scale bar: 10 μm) **B**. Relative fluorescence intensity of VAMP at the division plane during cell division. When the cells are treated with LatB, the accumulation of VAMP at the phragmoplast is strongly reduced; nevertheless accumulation is not completely inhibited by LatB. The dash line is at time 12, normally when the formation of the phragmoplast begins. But in this cell line, cell division seems to proceed faster. Error bar shows standard error of the mean, but in VAMP+100 μM LatB group, because there are only two cells recorded in this condition, the error bar shows the distribution of two cells.

To further evaluate the possibility that myosin XI was passively accumulating at the spindle because of its association with vesicles, I used the vesicle trafficking inhibitor, brefeldin A (BFA). When BFA was added to the moss cells, tip growth stopped, but surprisingly, not the initiation of cell division (**Figure 12**). Many of the tips started cell division, but they did not complete division as the cell plate could not expand normally (see **Figure 12**, 32 min panel). In these cells, myosin XI continued to accumulate on the spindle as well as at the phragmoplast; nevertheless, the localization of myosin XI at the division plane lasted longer than 1 hour.

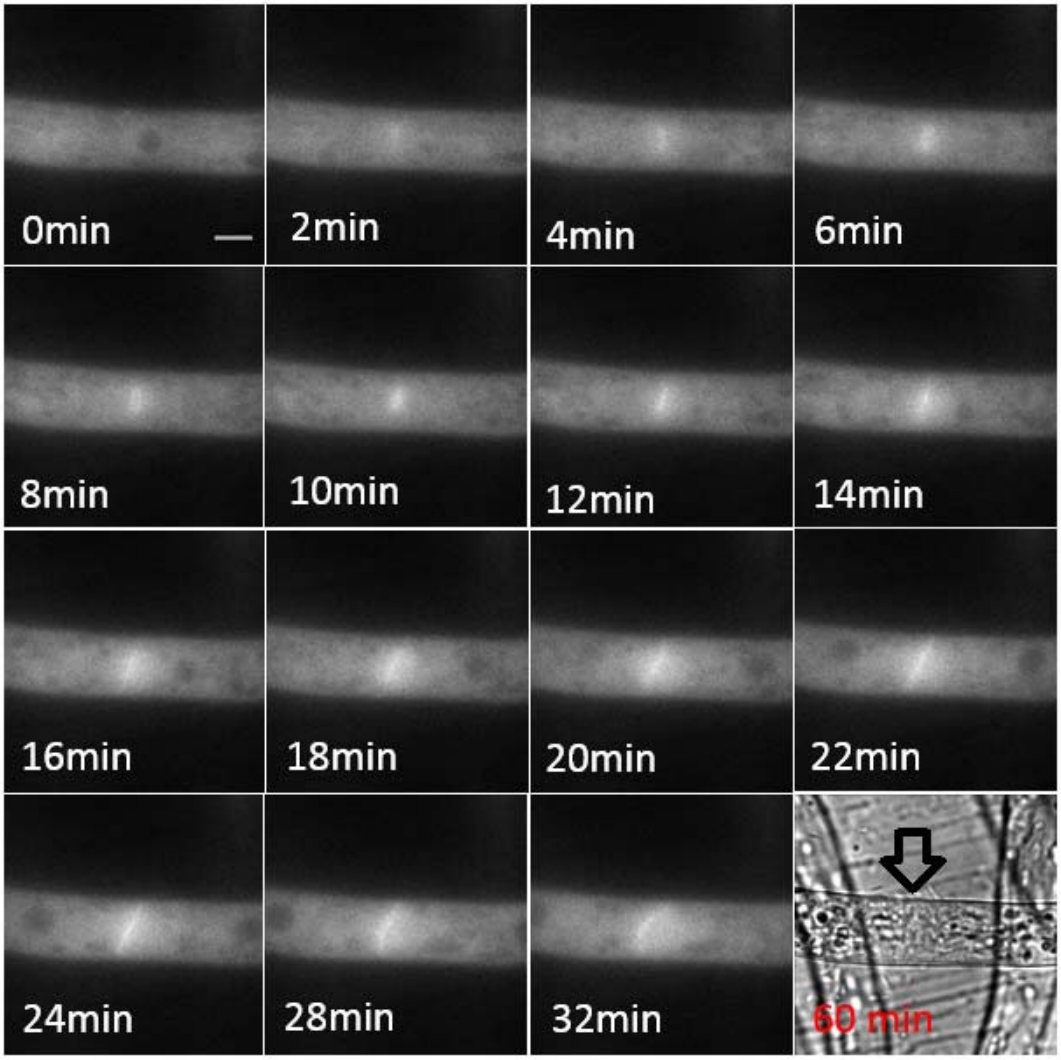

Figure 12. Representative example of the localization of myosin XI after brefeldin A treatment. Blocking vesicle trafficking does not affect the localization of myosin XI at the mitotic spindle and at the phragmoplast. However, since there are no vesicles supporting the expansion of the cell plate, myosin XI stays at the division plane much longer than under normal conditions. The bright field image from the last panel shows that even after 1 hr, the cell plate did not form at the division plane. Arrow indicates the division plane (Scale bar: 10 μm).

Together these results suggest that myosin XI accumulation on the mitotic spindle is not dependent on vesicles. As for the myosin XI at the phragmoplast, there is likely a fraction of myosin XI there that is not associated with vesicles.

3.4. Myosin XI and Endoplasmic Reticulum

The endoplasmic reticulum (ER) has been implicated in plant cell division and has been shown to associate with the mitotic spindle (Gupton et al., 2006); hence, I also tested the colocalization of myosin XI and the ER during *P. patens* cell division.

As shown in **Figure 13**, I found that the ER was present in the middle of the spindle in the first 2 min after nuclear envelope breakdown, but it quickly left the middle zone in the next 2 min. Using dual color imaging, I observed after 4 min, the center of the spindle had only increasing myosin XI signal, but not ER signal (**Figure 13B**). Thus there does not seem to be colocalization between the ER and myosin XI on the spindle after 2 min following nuclear envelope breakdown. However, when the phragmoplast formed at 12 min, I could detect that ER started accumulate along the newly formed cell plate close to the myosin XI signal. These observations suggest that myosin XI and ER can potentially associate at the phragmoplast; nevertheless, because of the limit of the resolution of my imaging method, I could not determine if myosin XI and the ER directly interact at the phragmoplast.

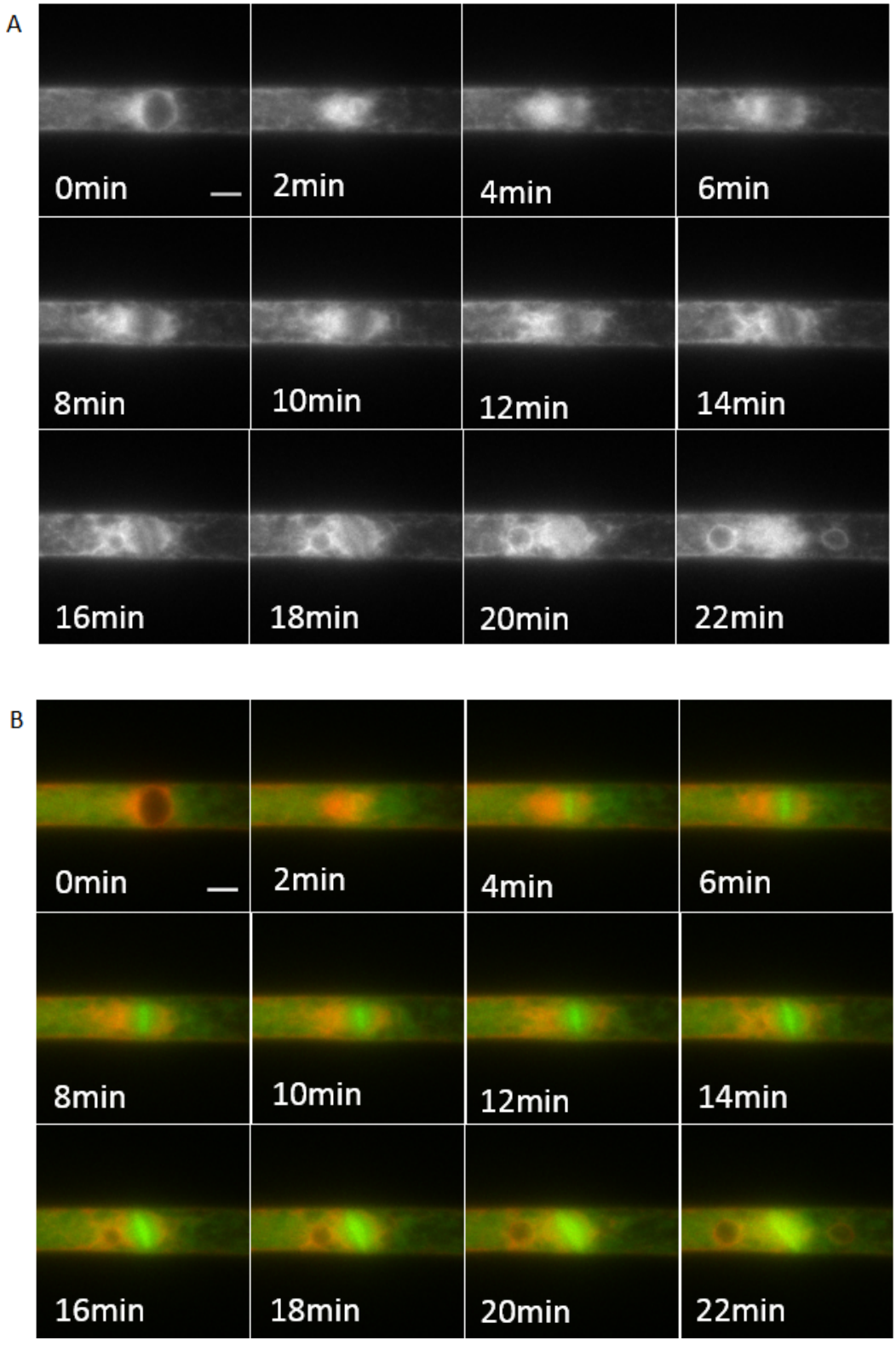

Figure 13. (Legend in the next page)

Figure 13. A representative example of the localization of ER during cell division. A. An example of the localization of ER during cell division. After the nuclear envelope breaks down at time 0, the ER briefly localized in the middle of the division plane before time 4 min, but soon leaves the middle of the spindle. After the formation of the phragmoplast at 12 min, the ER signal starts to appear at the division plane along the cell plate. **B**. Colocalization image of myosin XI-3mEGFP (green) and mCherry-ER (red). Myosin XI and the ER do not colocalize 4 min after nuclear envelope breakdown, but after the phragmoplast is formed, they colocalize at the cell plate. (Scale bar: 10 μm)

4. DISCUSSION

4.1. The Actin-independent Localization of Myosin XI

Based on my observations, myosin XI appears to have two accumulating events at the division plane during cell division. One happens shortly after nuclear envelope breakdown, localizing at the center of the spindle; the second one happens about 12 min later, following the formation of the phragmoplast, localizing along the cell plate.

In other plant systems, previous studies have shown F-actin localization on the mitotic spindle (Forer and Jackson, 1979; Seagull et al., 1987; Yasuda et al., 2005; Yu et al., 2006), as well as at the phragmoplast (Clayton and Lloyd, 1985), so I also looked at the localization of F-actin during cell division in *P. patens*. My results are similar to previous studies in that F-actin localized to the phragmoplast, but I could not detect a significant increase of F-actin on the spindle, which is consistent with results from a previous report of cell division in *P. patens* (Wu and Bezanilla, 2014). Because myosin XI is an actin-dependent motor, the presence of F-actin at the phragmoplast could explain the localization of myosin XI at same place, but the absence of actin accumulation on the spindle suggested a different actin-independent mechanism for accumulation of myosin XI in this structure. It is possible that I could not observe F-actin on the spindle because the concentration of actin on the spindle was below my detection limit, or because the F-actin on the spindle was too dynamic for lifeact-mEGFP to bind to it. If this is the case, and the localization of myosin XI is dependent on actin filaments during cell division, myosin XI accumulation should disappear when actin filaments are depolymerized.

Thus, to examine the relationships of actin filaments and myosin XI during cell division, I used the actin depolymerization drug, latrunculin B (LatB). At first, I used 200 µl of 10 µM

LatB, and saw that the tip cell stopped growing right after I added the drug, suggesting that there was a rapid inhibitory effect on F-actin. However, the cells continued to divide, though after division, some tip cells looked shorter than normal tip cells. In these post mitotic cells, I found that the localization of actin was totally disrupted: there was no clear accumulation of actin anywhere in the cell. Surprisingly, in the presence of LatB, I was still able to detect accumulation of myosin XI on the spindle and at the phragmoplast. The increase of myosin XI at the phragmoplast was partically affected by the drug, but I still saw a clear increase of myosin XI signal at the phragmoplast. A possible difficulty with this 10 μM LatB concentration was that there might not be enough drug present to prevent actin filament formations during cell division, as I could identify cells containing actin/myosin XI ectopic clusters similar to those detected when cells are treated with 10 μM concentration of LatB (Furt et al., 2013). So I increased the concentration of LatB to 100 μM and used 500 μl of it. Again, even at this higher concentration, I could detect the accumulation of myosin XI at both places, while there was no actin accumulation or the presence of ectopic clusters. Based on these results, and consistent with the previous studies (Wu and Bezanilla, 2014), I can conclude that actin is not essential for cell division in the protonemata of *P. patens*, and that the accumulation of myosin XI on the spindle is not actin dependent, while the accumulation of myosin XI at the phragmoplast is partially dependent on actin filaments.

4.2. Myosin XI May not Be a Passive Passenger on the Mitotic Spindle

The initial hypothesis I tested to explain the actin-independent behavior of myosin XI was that because myosin XI attaches to many vesicles and organelles in plant cells, these myosin XI molecules might simply be a passive passenger, brought to these locations by vesicles and organelles.

If myosin XI was brought to these locations passively, I should be able to find myosin XI colocalizing with vesicles or organelles. So I used double fluorescently labeled moss lines to verify if there was any colocalization of myosin XI and vesicles or organelles on the spindle and at the phragmoplast. Initially, I imaged myosin XI and a vesicle marker, the v-SNARE vesicle-associated membrane protein (VAMP). As reported by other groups (Zhang et al., 2011), VAMP accumulated at the phragmoplast, but not on the spindle. I concluded that VAMP-containing vesicles are not good candidates for the vehicle that brings myosin XI to the spindle.

Interestingly, when I used LatB to depolymerize actin filaments, I saw a clear decrease of VAMP signal at the phragmoplast, but the VAMP signal was not completely lost, which was similar to the case of myosin XI.

Given the similar effect of LatB treatment on myosin XI and VAMP accumulation at the phragmoplast, it is possible that there are two types of VAMP-labeled vesicles and two populations of myosin XI. Alternatively, VAMP-labeled vesicles could have both myosin XI and kinesins attached, which allows them to move along both cytoskeletal elements.

The following scenarios could explain the decrease of signals of myosin XI and VAMP labeled vesicles. One is that actin and myosin XI are responsible for accumulating of some of the vesicles to the cell plate directly. However, this actin-dependent vesicle accumulation is probably not essential for cell plate expansion; otherwise the expansion would be slower in the absence of F-actin, as cells would not have enough vesicles to sustain normal cell plate expansion. Instead, when I compared the time between nuclear envelope breakdowns and the cell plate attachment to side membranes, I did not find a huge difference; both occurred around 28 min in the presence or absence of F-actin. This observation is consistent with a previous report from another group

which showed that cell division proceeds at a normal rate after depolymerizing actin filaments (Gupton et al., 2006).

A different possibility is that the transport of vesicles in other parts of the cell is actin dependent, but the accumulation of these vesicles at the phragmoplast is not. Thus, when I depolymerized actin filaments, the numbers of vesicles that could reach the phragmoplast decreased, resulting in a decreased VAMP signal. I believe this scenario is also unlikely, because it does not explain that the duration of cell division is not altered when F-actin is absent as the diffusion of these vesicles might not be fast enough to satisfy the requirement for vesicles for normal cell plate expansion.

A third more likely possible explanation is that actin is participating in the transport and recycling of vesicles at the cell plate. When actin filaments are absent, both the transport of vesicles towards the phragmoplast and the recycling of vesicles from the cell plate are stopped, thus, the increase of membrane at the phragmoplast maintains normal speed, though there might be small defects that I am not able to detect in this study. Further investigations, ideally using super resolution or electron microscopy, are needed to determine the function of actin during plant cell division.

In addition to VAMP as a vesicle marker, I also examined the localization of RabA proteins, which are known to associate with vesicles (Qi and Zheng, 2011). We checked two types of RabAs in *P. patens* (Agar), and found that they all behave similarly to VAMPs; i.e., they did not colocalize with myosin XI on the mitotic spindle but they did accumulate at the phragmoplast. Thus, RabA-containing vesicles might not participate in the mechanism that brings myosin XI to the spindle. When I compared the increase in levels of different RabA proteins, I found they accumulated differently. From these observations, it seems that

protonemata cells selectively accumulate different vesicles into the cell plate to meet the needs for proper cell plate expansion. However, determining whether the localization of RabA-containing vesicles is partially dependent on actin filament, just like VAMP containing vesicles, will require future testing with LatB treatments.

To further investigate the relationship between myosin XI and vesicle trafficking, I used the vesicle trafficking inhibitor, brefeldin A (BFA), which has been used for many years to inhibit vesicle trafficking to the Golgi apparatus (Misumi et al., 1986; Yasuhara and Shibaoka; Lam et al., 2009). After adding BFA, tip cells stopped growing immediately, which indicates that the inhibitor is active in protonemata. Surprisingly, I was able to find cells that started cell division; however, these tip cells failed to complete cell division, because of failure of cell plate expansion. In these cells, I was still able to detect the accumulation of myosin XI on the spindle and the initial accumulation at the phragmoplast, though the signal of myosin XI at the phragmoplast did not increase as the phragmoplast and the cell plate failed to expand. But after I finished imaging, I could always find some cells with a strong myosin XI signal at the phragmoplast. These tip cells were very short as cell growth was arrested at the beginning, but they still could form the cell plate quite well. I think this was because different cells were exposed to the drug unevenly, with some having less than others, and also because BFA gradually loses its function due to the metabolism of this drug by the cells (Fujiwara et al., 1988). In future experiments, it will be important to find a higher concentration of BFA or a method of applying the drug that results in more consistent results. It will also be important to verify that I blocked all vesicle trafficking towards the phragmoplast, this could be done combining BFA treatment with the imaging of the vesicle markers discussed above.

These observations suggest that myosin XI is not attached to vesicles on the spindle. To further explore the mechanism of myosin XI localization to the spindle, I investigated the possibility that myosin XI was associated with the endoplasmic reticulum. The reason for this is that it has previously been reported that the ER is involved in cell division in plants (Gupton et al., 2006). To address this, I constructed a moss line with EGFP-labeled myosin XI and mCherry-labeled ER. In this line, I detected that the ER reached the center of the newly formed spindle, but it quickly left the middle zone, and in the following minutes, I could only detect the green signal of myosin XI there. It is possible that the initial accumulation of myosin XI in the spindle was directed by the ER, but this seems unlikely because the ER does not continue to accumulate in the middle zone. Following the formation of the phragmoplast, I was able to see the localization of the ER signal along the phragmoplast. However, due to the resolution of my movies I was not able to determine if myosin and the ER were interacting.

Together, these results suggest that myosin XI is not a passive passenger on the mitotic spindle, and that myosin XI may have some novel function during cell division.

4.3. Possible Actin-independent Roles of Myosin XI During Cell Division.

Having examined the colocalization of myosin XI, two types of vesicle marker and the ER, and also after using a vesicle trafficking inhibitor to investigate the relationship between myosin XI and Golgi-derived vesicles, I think it is unlikely that myosin XI is passively transported to the spindle and the phragmoplast by vesicles or the ER. In this following section, I will explore other possibilities because there are many previous studies indicating myosins could have interesting functions not associated with actin (Lantz and Miller, 1998; Wu et al., 1998; Doyle et al., 2009).

One possibility is that myosin XI interacts with microtubules. There are some studies indicating this could be the case. For example, in 1998, Wu *et al.* showed that in mouse cells, myosin Va colocalized with microtubule organizing center (MTOC) without detectable F-actin on the spindle (Wu et al., 1998), and they also showed that this colocalization was not specific to mouse cells, as they also stained human cells (HeLa), and they still observed the localization of myosin Va at the MTOC. Similarly, Doyle showed in fission yeast that a class V myosin, myo51p could associate with spindle pole bodies (Doyle et al., 2009); they found that this association was independent of actin, but interestingly, dependent on stable microtubule networks. Since myosin XI and myosin V are homologues, it is possible they share the same ability to interact with microtubules.

Another similar possibility is that myosin XI associates with microtubules through microtubule associated proteins (MAPs). Supporting evidence for this possibility was reported in *Drosophila* embryos (Lantz and Miller, 1998). Lantz *et al.* found that a class VI unconventional myosin was coexpressed with a microtubule binding protein in several tissues, and they colocalized to the same structures. They thought this interaction between myosin VI and the microtubule binding protein might help coordinate the interaction between microtubules and microfilaments. Furthermore, this reported interaction suggests that the interaction between myosins and microtubule binding proteins is possible. If this is the case in *P. patens*, in the future, I should be able to identify microtubule binding proteins that could interact with myosin XI during cell division.

An alternative possibility is that myosin XI interacts with nuclear envelope proteins on the spindle and different structures at the phragmoplast. Tamura *et al.* showed that in *Arabidopsis*, one component in the linker of nucleoskeleton and cytoskeleton (LINC) complex, WIT1, could

interact with myosin XI-i (Tamura et al., 2013). In addition, a previous report showed that another protein in this complex localizes at the middle of the spindle during metaphase (Graumann and Evans, 2011). Hence this association could be the way in which myosin XI is brought to the spindle in *P. patens* - through the connection with the LINC complex. Though this is possible, I anticipate the other two alternative possibilities I mentioned above are more likely for the following reasons: 1. During telophase, the LINC complex moves towards the cell poles with the chromosomes, while myosin XI appears to stay in the middle; 2. The association with the LINC complex does not explain the localization of myosin XI at the phragmoplast, as the LINC complex does not localizate there; 3. The association with the LINC complex still does not explain the function of myosin XI on the spindle, unless myosin XI interacts with other proteins besides F-actin. So if the LINC complex plays a role in bringing myosin XI to the spindle, there must be something else helping maintain the concentration of myosin XI at the midzone throughout cell division, and helping accumulate myosin XI at the phragmoplast.

Since I was not able to find anything that colocalizes well with myosin XI on the spindle, it is hard for me to definitely state the function of myosin XI at the spindle or what myosin XI is associating with on the spindle. But after researching the literature, I was able to propose three possibilities as listed above. Furthermore, I think all these possibilities are not mutually exclusive; myosin XI could interact with microtubules or microtubule associated proteins to help regulate the formation of the spindle and the phragmoplast, or it could also help localize the LINC complex or similar structures to the middle of the spindle during metaphase through its interaction with both LINC complex and microtubules. To have a better understanding of myosin XI during cell division, more studies, such as myosin XI co-immunoprecipitations, are required, looking closer at its localization during cell division in plant cells.

4.4. Similarity of the Localizations of Myosin XI and Myosin VIII

As showed by Wu and Bezanilla (Wu and Bezanilla, 2014), myosin VIII accumulates at the center of the spindle as well as at the phragmoplast, even in the absence of F-actin. Based on my data, it appears that myosin XI has the same localization as myosin VIII during cell division. Nevertheless, these two proteins have different functions during interphase in *P. patens* (Vidali et al., 2010; Wu et al., 2011). Furthermore, we do not have simultaneous imaging of both molecules, which makes a side-by-side comparison difficult. I was not able to identify any previous work using direct comparisons for the participation of these two myosins in other plant systems during cell division. Thus future comparison will require higher resolution images of myosin XI and the simultaneous localization of these two important proteins.

An alternative way to address this problem is to look into the similarities between myosin XI and VIII, trying to identify something in common that could explain their similar behavior during cell division. Though I did not look at the sequence similarity across the complete molecules, myosin XI and myosin VIII both share an N-terminal SH3-like domain (See **Figure I.3**) (Thompson and Langford, 2002). Among the myosin superfamily, only myosin II, myosin VIII and myosin XI have this SH3-like domain at their N-terminus, and the function of this SH3-like domain is unknown in plant myosins. Thus I suggest that this domain might be one possible reason that myosin VIII and myosin XI share a similar behavior during cell division.

SH3 domain stands for the Src homology 3 domain, which is widely present in all eukaryotes. It is known as an important protein-interaction module, typically binding to proline-rich peptides. In animal cells, many microtubule-associated proteins have these proline-rich peptides that could interact with other proteins with SH3 domains (Sontag et al., 2012).

Currently, little is known about plant microtubule-associated proteins, but in the future, we may be able to identify some microtubule-associated proteins with proline-rich peptides that can interact with myosin XI and VIII.

Based on the N-terminal similarity of myosin XI and myosin VIII, and the importance of SH3 domain in protein-protein interaction, I think these myosins could interact with microtubules indirectly through the interaction between SH3-like domains and microtubule associated proteins, in a way illustrated in **Figure IV.1**. In the case of MAP65, it has been shown that MAP65 could work as a spring system to control the length of the overlapping part of two anti-parallel microtubules (Lansky et al., 2015). It is possible that by using myosin, plant cell could potentially gain several benefits: 1. Because myosin is usually bigger than MAPs (for instance, in tobacco, MAP65 is about 65kD in size (Smertenko et al., 2000), while myosin XI is about 175kD in size), the incorporation of myosin XI in the MAP "spring" system could reduce the number of MAP molecules required to get a similar effect; 2. Because myosin XI is abundant in the plant cytoplasm, cells do not need to synthesize more molecules and could simply recruit what is diffusing in the cytoplasm; 3. the incorporation of myosin XI may control the distance between two MAP molecules, providing finer control of microtubule organization in both the spindle and the phragmoplast.

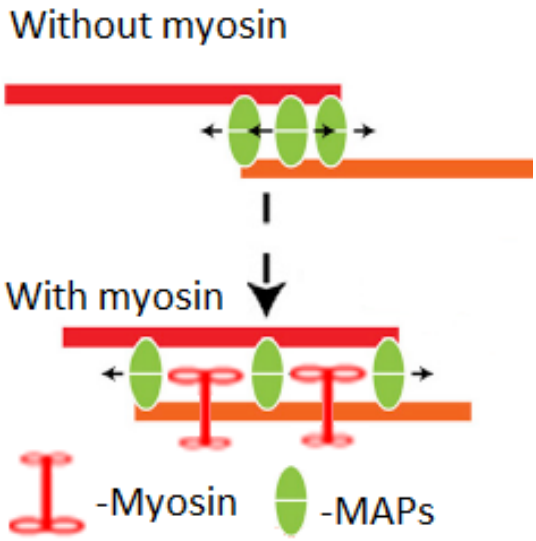

Figure IV.1. Possible interaction between myosin and MAPs. Modified from (Lansky et al., 2015). Some microtubule associated proteins stay at the overlapping site of two anti-parallel microtubule filaments, regulating the length of the overlapping site. When myosin is present, myosin might interact with MAPs and increase the distance between two MAPs, helping control the formation of the microtubule structure.

4.5. Difficulties in Determining the Functions of Actin and Myosins During Cell Division

Because the spindle and the phragmoplast are usually described as microtubule structures, studies on these structures are dominated by research on microtubules, microtubule motors and microtubule-associated proteins. Not many reports are focused on studying actin and myosins during plant cell division. However, I was still able to find several articles where the presence of actin and myosins on the spindles was investigated with different methods (Forer and Jackson, 1979; Seagull et al., 1987; Yasuda et al., 2005; Yu et al., 2006) as well as the presence of actin at the phragmoplast (Clayton and Lloyd, 1985; Molchan et al., 2002).

Unfortunately, the importance of F-actin and myosin on the spindle and at the phragmoplast are still under debate. Some groups have shown there is localization of F-actin on

the spindle, while others have not shown localization of actin on the spindle at all (Barak et al., 1981; Sommi et al., 2011). Even if researchers agreed with the presence of actin and myosin on these structures, to determine the functions of these proteins is even more difficult.

There are several major problems we face to understand the function of actin and myosins during cell division (Sandquist et al., 2011). The first problem is the existence of reports with different results obtained with the same drug treatments (Sampson and Pickett-Heaps, 2001; Yasuda et al., 2005); further complicating this problem is that even with the same drug in the same species, researchers get different results (Fabian and Forer, 2007; Xie and Forer, 2008). A separate problem is that because biological processes are usually interconnected, it is hard to tell whether a given abnormality is the indirect result of inhibiting a separate off-target process. Similarly, actin and myosins are important in many biological processes, and we have no drugs that can affect participating in a single process; when we treat the cells with drugs, it is hard to determine whether the abnormality is caused by the specific portion of actin / myosins at specific places at specific time.

5. CONCLUSIONS AND FUTURE DIRECTIONS

5.1. Major Conclusions

The results from this thesis indicate that in *P. patens*, after the nuclear envelope breaks down, myosin XI accumulates in the middle of the division plane, where the spindle localizes. This myosin XI localization is not dependent on actin filaments. So far, I could not find anything that colocalizes well with myosin XI on the spindle, thus I think myosin XI might have some novel functions that are independent of actin and are likely associated with microtubules.

After the formation of the phragmoplast at about time 12 min, myosin XI stays along the cell plate and keeps accumulating as the cell plate expands toward the periphery. This myosin XI localization is partially actin-dependent. In addition to myosin XI, I also found vesicle markers, such as VAMPs and RabAs, that accumulate along the cell plate as well, and it appears the accumulation of these vesicles is partially actin-dependent, similar to myosin XI, indicating that actin plays a role in accumulating myosin XI and these vesicles at the division plane, though it is not critical for the normal cell plate expansion.

Besides myosin XI and vesicles, I also tested the potential participation of the endoplasmic reticulum in *P. patens* cell division. ER stays around the spindle 4 min after the nuclear envelope breaks down, thus having no colocalization with myosin XI on the spindle. However, after the phragmoplast is formed, the ER signal appears along the cell plate, suggesting the involvement of ER in the formation of the cell plate. But because of the resolution of my movies, I could not tell if the ER is truly interacting with myosin XI or not.

In summary, my work is the first attempt to show the localization of myosin XI in plant cell division, and shows the actin-independent localization of myosin XI. My results leave us with

new questions that require future research. This research of myosin XI in plant cell division will help us better understand this important motor, and ideally, it should enable us to control this motor protein to accomplish specific goals, such as accelerating plant cell growth and possibly increasing the yield of crops.

5.2. Future Directions

One of the major problems in this project is that I do not have enough sample numbers for the statistical analysis of some lines and treatments. More tests with these lines and drug treatments will strengthen the conclusions of this work.

All my data was not acquired with high a resolution imaging method, because I had no experience investigating plant cell division. Initially, I wanted to record as many cells as possible so I might be able to get one or two division events. In order to detect finer structures and gain better localization information, I need to find ways to improve the quality of my acquired data, as well as to use a higher resolution method. One possible direction is to use image deconvolution to gain better localization information, which will reduce the out of focus background. Because I used epifluorescence microscopy, the out-focus light reduces the signal-to-noise ratio in my images. Although I can get a general idea of the localization of my labeled proteins, I cannot get more precise localizations of them. This is more critical when I try to image a structure as complex as the ER. Another direction is to use a different imaging method, for example a spinning-disc confocal microscope. Now that I have more experience and confidence recording plant cell division, I should be able to obtain much higher quality images and show more information about the localizations of the proteins I have been investigating.

In addition to improving my movies and imaging method, I also would try to test the function of myosin XI. Since our lab already has a a myosin XI temperature sensitive line, I could try to disrupt the function of myosin XI during cell division by increasing the temperature when the cell starts dividing and see how plant cell division is affected. However, one major problem we have is we are not sure if the functional part of myosin XI during cell division is the part we mutated. If not, we need to try to make other mutants, such as a mutant lacking the SH3 domain. The other way to test the function of myosin XI is try to use a myosin inhibitor, like 2,3-Butanedione monoxime (BDM), which affects the ATP binding site on myosins. Unfortunately this inhibitor is known to have low specificity.

To test the interaction between myosin XI and some other proteins, I suggest using an co-immunoprecipitation assay. First, I would try to find an optimized procedure to lyses plant cells. After that, I would attach an anti-myosin XI antibody to beads, and pull down myosin XI, along with proteins that interact with myosin XI, in *P. patens*. Next, I would elute protein-protein interaction complex and use mass spectrometry to determine what is interacting with myosin XI. As we are interested in protein-protein interaction during cell division, before lysing the plant cells, I would also try to synchronize *P. patens* cell (Lucretti and Dolezel, 1995) and only lyse cells when most of cells are dividing.

I could also try to do some tests based on my hypothesis on the interactions of myosin XI and microtubules. One way to do this is to make a double-labeled line and use better imaging methods to detect the localizations of myosin XI and microtubules with high resolution. Meanwhile, I could also try some in vitro tests with purified myosin XI and microtubules. If I could detect the interaction of myosin XI and microtubules, and figure out the effect of myosin

XI on the microtubules *in vitro*, I could conclude that one of the functions of myosin XI during cell division really is regulating microtubules.

In addition, I could also try to detect the colocalization of myosin XI and some microtubule binding proteins, using double-labeled lines or *in vitro* binding assays, starting with the proteins reported in the literature. For example, MAP65 has been studied in *P. patens* during cell division, and it localizes to similar places as myosin XI during cell division (Kosetsu et al., 2013), thus I could start with MAP65.I would use the RNAi construct developed by Kosetsu et al. (Kosetsu et al., 2013); if the localization of myosin XI is altered by RNAi, I could conclude that the localization of myosin XI is dependent on MAP65.

To further test the importance of the SH3-like domain I mentioned before, I would also use inducible promoters to express mEGFP-labeled SH3-like domain from myosin XI into *P. patens* protonemata cells during cell division, if this SH3-like domain construct accumulates at the same position as myosin XI does, I would conclude the SH3-like domain is probably responsible for the localization of myosin XI during plant cell division. Alternatively, I could also use the same methods to express mEGFP-labeled myosin XI lacking SH3-like domain during cell division to confirm whether SH3-like domain is important for the localization of the localization of myosin XI at the mitotic spindle and the phragmoplast.

6. REFERENCES

Agar, E. (2013). Interactions between myosin XIa and rab proteins in the moss *Physcomitrella patens*. BS. Senior Thesis (Major Qualifying Project), Worcester Polytechnic Institute. Advisor: L. Vidali

Ambrose, J.C., and Wasteneys, G.O. (2008). CLASP modulates microtubule-cortex interaction during self-organization of acentrosomal microtubules. Mol Biol Cell **19,** 4730-4737.

Ambrose, J.C., Li, W., Marcus, A., Ma, H., and Cyr, R. (2005). A minus-end-directed kinesin with plus-end tracking protein activity is involved in spindle morphogenesis. Mol Biol Cell **16,** 1584-1592.

Avisar, D., Prokhnevsky, A.I., and Dolja, V.V. (2008). Class VIII myosins are required for plasmodesmatal localization of a closterovirus Hsp70 homolog. J Virol **82,** 2836-2843.

Baluska, F., Cvrckova, F., Kendrick-Jones, J., and Volkmann, D. (2001). Sink plasmodesmata as gateways for phloem unloading. Myosin VIII and calreticulin as molecular determinants of sink strength? Plant Physiol **126,** 39-46.

Bannigan, A., Lizotte-Waniewski, M., Riley, M., and Baskin, T.I. (2008). Emerging molecular mechanisms that power and regulate the anastral mitotic spindle of flowering plants. Cell Motil Cytoskeleton **65,** 1-11.

Bannigan, A., Scheible, W.R., Lukowitz, W., Fagerstrom, C., Wadsworth, P., Somerville, C., and Baskin, T.I. (2007). A conserved role for kinesin-5 in plant mitosis. J Cell Sci **120,** 2819-2827.

Barak, L.S., Nothnagel, E.A., DeMarco, E.F., and Webb, W.W. (1981). Differential staining of actin in metaphase spindles with 7-nitrobenz-2-oxa-1,3-diazole-phallacidin and fluorescent DNase: is actin involved in chromosomal movement? Proc Natl Acad Sci U S A **78,** 3034-3038.

Bezanilla, M., Forsburg, S.L., and Pollard, T.D. (1997). Identification of a second myosin-II in *Schizosaccharomyces pombe*: Myp2p is conditionally required for cytokinesis. Mol Biol Cell **8,** 2693-2705.

Bezanilla, M., Perroud, P.F., Pan, A., Klueh, P., and Quatrano, R.S. (2005). An RNAi system in *Physcomitrella patens* with an internal marker for silencing allows for rapid identification of loss of function phenotypes. Plant Biol (Stuttg) **7,** 251-257.

Bi, E.F., and Lutkenhaus, J. (1991). FtsZ ring structure associated with division in *Escherichia coli*. Nature **354,** 161-164.

Binarova, P., Dolezel, J., Draber, P., Heberle-Bors, E., Strnad, M., and Bogre, L. (1998). Treatment of Vicia faba root tip cells with specific inhibitors to cyclin-dependent kinases leads to abnormal spindle formation. Plant J **16,** 697-707.

Binarova, P., Cenklova, V., Prochazkova, J., Doskocilova, A., Volc, J., Vrlik, M., and Bogre, L. (2006). Gamma-tubulin is essential for acentrosomal microtubule nucleation and coordination of late mitotic events in *Arabidopsis*. Plant Cell **18,** 1199-1212.

Boevink, P., Oparka, K., Santa Cruz, S., Martin, B., Betteridge, A., and Hawes, C. (1998). Stacks on tracks: the plant Golgi apparatus traffics on an actin/ER network. Plant J **15,** 441-447.

Bramhill, D. (1997). Bacterial cell division. Annu Rev Cell Dev Biol **13,** 395-424.

Bramhill, D., and Thompson, C.M. (1994). GTP-dependent polymerization of *Escherichia coli* FtsZ protein to form tubules. Proc Natl Acad Sci U S A **91,** 5813-5817.

Cassimeris, L. (1999). Accessory protein regulation of microtubule dynamics throughout the cell cycle. Curr Opin Cell Biol **11,** 134-141.

Chan, J., Calder, G., Fox, S., and Lloyd, C. (2005). Localization of the microtubule end binding protein EB1 reveals alternative pathways of spindle development in *Arabidopsis* suspension cells. Plant Cell **17,** 1737-1748.

Chang-Jie, J., and Sonobe, S. (1993). Identification and preliminary characterization of a 65 kDa higher-plant microtubule-associated protein. J Cell Sci **105 (Pt 4),** 891-901.

Chow, C.M., Neto, H., Foucart, C., and Moore, I. (2008). Rab-A2 and Rab-A3 GTPases define a trans-golgi endosomal membrane domain in *Arabidopsis* that contributes substantially to the cell plate. Plant Cell **20,** 101-123.

Clayton, L., and Lloyd, C.W. (1985). Actin organization during the cell cycle in meristematic plant cells. Actin is present in the cytokinetic phragmoplast. Exp Cell Res **156,** 231-238.

Cleary, A.L., and Smith, L.G. (1998). The Tangled1 gene is required for spatial control of cytoskeletal arrays associated with cell division during maize leaf development. Plant Cell **10,** 1875-1888.

Cope, M.J., Whisstock, J., Rayment, I., and Kendrick-Jones, J. (1996). Conservation within the myosin motor domain: implications for structure and function. Structure **4,** 969-987.

Dai, K., and Lutkenhaus, J. (1991). ftsZ is an essential cell division gene in *Escherichia coli*. J Bacteriol **173,** 3500-3506.

Desai, A., Verma, S., Mitchison, T.J., and Walczak, C.E. (1999). Kin I kinesins are microtubule-destabilizing enzymes. Cell **96,** 69-78.

Dhonukshe, P., and Gadella, T.W., Jr. (2003). Alteration of microtubule dynamic instability during preprophase band formation revealed by yellow fluorescent protein-CLIP170 microtubule plus-end labeling. Plant Cell **15,** 597-611.

Dhonukshe, P., Vischer, N., and Gadella, T.W., Jr. (2006). Contribution of microtubule growth polarity and flux to spindle assembly and functioning in plant cells. J Cell Sci **119,** 3193-3205.

Dhonukshe, P., Mathur, J., Hulskamp, M., and Gadella, T.W., Jr. (2005). Microtubule plus-ends reveal essential links between intracellular polarization and localized modulation of endocytosis during division-plane establishment in plant cells. BMC Biol **3,** 11.

Dixit, R., and Cyr, R.J. (2002). Spatio-temporal relationship between nuclear-envelope breakdown and preprophase band disappearance in cultured tobacco cells. Protoplasma **219,** 116-121.

Doyle, A., Martin-Garcia, R., Coulton, A.T., Bagley, S., and Mulvihill, D.P. (2009). Fission yeast Myo51 is a meiotic spindle pole body component with discrete roles during cell fusion and spore formation. J Cell Sci **122,** 4330-4340.

El Kasmi, F., Krause, C., Hiller, U., Stierhof, Y.D., Mayer, U., Conner, L., Kong, L., Reichardt, I., Sanderfoot, A.A., and Jurgens, G. (2013). SNARE complexes of different composition jointly mediate membrane fusion in *Arabidopsis* cytokinesis. Mol Biol Cell **24,** 1593-1601.

Erickson, H.P., Taylor, D.W., Taylor, K.A., and Bramhill, D. (1996). Bacterial cell division protein FtsZ assembles into protofilament sheets and minirings, structural homologs of tubulin polymers. Proc Natl Acad Sci U S A **93,** 519-523.

Fabian, L., and Forer, A. (2007). Possible roles of actin and myosin during anaphase chromosome movements in locust spermatocytes. Protoplasma **231,** 201-213.

Fache, V., Gaillard, J., Van Damme, D., Geelen, D., Neumann, E., Stoppin-Mellet, V., and Vantard, M. (2010). Arabidopsis kinetochore fiber-associated MAP65-4 cross-links microtubules and promotes microtubule bundle elongation. Plant Cell **22,** 3804-3815.

Forer, A., and Jackson, W.T. (1979). Actin in spindles of *Haemanthus katherinae* endosperm. I. General results using various glycerination methods. J Cell Sci **37,** 323-347.

Fujiwara, T., Oda, K., Yokota, S., Takatsuki, A., and Ikehara, Y. (1988). Brefeldin A causes disassembly of the Golgi complex and accumulation of secretory proteins in the endoplasmic reticulum. J Biol Chem **263,** 18545-18552.

Furge, K.A., Wong, K., Armstrong, J., Balasubramanian, M., and Albright, C.F. (1998). Byr4 and Cdc16 form a two-component GTPase-activating protein for the Spg1 GTPase that controls septation in fission yeast. Current Biology **8,** 947-954.

Furt, F., Liu, Y.C., Bibeau, J.P., Tüzel, E., and Vidali, L. (2013). Apical myosin XI anticipates F-actin during polarized growth of *Physcomitrella patens* cells. Plant J **73,** 417-428.

Furusawa, T., Ikawa, S., Yanai, N., and Obinata, M. (2000). Isolation of a novel PDZ-containing myosin from hematopoietic supportive bone marrow stromal cell lines. Biochem Biophys Res Commun **270,** 67-75.

Gadde, S., and Heald, R. (2004). Mechanisms and molecules of the mitotic spindle. Curr Biol **14,** R797-805.

Gaillard, J., Neumann, E., Van Damme, D., Stoppin-Mellet, V., Ebel, C., Barbier, E., Geelen, D., and Vantard, M. (2008). Two microtubule-associated proteins of *Arabidopsis* MAP65s promote antiparallel microtubule bundling. Mol Biol Cell **19,** 4534-4544.

Gerisch, G., and Weber, I. (2000). Cytokinesis without myosin II. Curr Opin Cell Biol **12,** 126-132.

Glotzer, M. (2001). Animal cell cytokinesis. Annu Rev Cell Dev Biol **17,** 351-386.

Golomb, L., Abu-Abied, M., Belausov, E., and Sadot, E. (2008). Different subcellular localizations and functions of *Arabidopsis* myosin VIII. BMC Plant Biol **8,** 3.

Graumann, K., and Evans, D.E. (2011). Nuclear envelope dynamics during plant cell division suggest common mechanisms between kingdoms. Biochem J **435,** 661-667.

Gruss, O.J., Wittmann, M., Yokoyama, H., Pepperkok, R., Kufer, T., Sillje, H., Karsenti, E., Mattaj, I.W., and Vernos, I. (2002). Chromosome-induced microtubule assembly mediated by TPX2 is required for spindle formation in HeLa cells. Nat Cell Biol **4,** 871-879.

Gunning, B.E., and Wick, S.M. (1985). Preprophase bands, phragmoplasts, and spatial control of cytokinesis. J Cell Sci Suppl **2,** 157-179.

Gupton, S.L., Collings, D.A., and Allen, N.S. (2006). Endoplasmic reticulum targeted GFP reveals ER organization in tobacco NT-1 cells during cell division. Plant Physiol Biochem **44,** 95-105.

Hepler, P.K., and Jackson, W.T. (1968). Microtubules and early stages of cell-plate formation in the endosperm of Haemanthus katherinae Baker. J Cell Biol **38,** 437-446.

Hepler, P.K., Valster, A., Molchan, T., and Vos, J.W. (2002). Roles for kinesin and myosin during cytokinesis. Philos Trans R Soc Lond B Biol Sci **357,** 761-766.

Hiwatashi, Y., Sato, Y., and Doonan, J.H. (2014). Kinesins have a dual function in organizing microtubules during both tip growth and cytokinesis in *Physcomitrella patens*. Plant Cell **26,** 1256-1266.

Hiwatashi, Y., Obara, M., Sato, Y., Fujita, T., Murata, T., and Hasebe, M. (2008). Kinesins are indispensable for interdigitation of phragmoplast microtubules in the moss *Physcomitrella patens*. Plant Cell **20,** 3094-3106.

Ho, C.M., Hotta, T., Kong, Z., Zeng, C.J., Sun, J., Lee, Y.R., and Liu, B. (2011). Augmin plays a critical role in organizing the spindle and phragmoplast microtubule arrays in *Arabidopsis*. Plant Cell **23,** 2606-2618.

Hong, Z., Delauney, A.J., and Verma, D.P. (2001). A cell plate-specific callose synthase and its interaction with phragmoplastin. Plant Cell **13,** 755-768.

Hoshino, H., Yoneda, A., Kumagai, F., and Hasezawa, S. (2003). Roles of actin-depleted zone and preprophase band in determining the division site of higher-plant cells, a tobacco BY-2 cell line expressing GFP-tubulin. Protoplasma **222,** 157-165.

Hotta, T., Haraguchi, T., and Mizuno, K. (2007). A novel function of plant histone H1: microtubule nucleation and continuous plus end association. Cell Struct Funct **32,** 79-87.

Hotta, T., Kong, Z., Ho, C.M., Zeng, C.J., Horio, T., Fong, S., Vuong, T., Lee, Y.R., and Liu, B. (2012). Characterization of the Arabidopsis augmin complex uncovers its critical function in the assembly of the acentrosomal spindle and phragmoplast microtubule arrays. Plant Cell **24,** 1494-1509.

Huisman, S.M., Bales, O.A., Bertrand, M., Smeets, M.F., Reed, S.I., and Segal, M. (2004). Differential contribution of Bud6p and Kar9p to microtubule capture and spindle orientation in *S. cerevisiae*. J Cell Biol **167,** 231-244.

Ito, K., Ikebe, M., Kashiyama, T., Mogami, T., Kon, T., and Yamamoto, K. (2007). Kinetic mechanism of the fastest motor protein, *Chara* myosin. J Biol Chem **282,** 19534-19545.

Jurgens, G. (2005a). Plant cytokinesis: fission by fusion. Trends Cell Biol **15,** 277-283.

Jurgens, G. (2005b). Cytokinesis in higher plants. Annu Rev Plant Biol **56,** 281-299.

Kawamura, E., and Wasteneys, G.O. (2008). MOR1, the *Arabidopsis thaliana* homologue of Xenopus MAP215, promotes rapid growth and shrinkage, and suppresses the pausing of microtubules in vivo. J Cell Sci **121,** 4114-4123.

Kitayama, C., Sugimoto, A., and Yamamoto, M. (1997). Type II myosin heavy chain encoded by the myo2 gene composes the contractile ring during cytokinesis in *Schizosaccharomyces pombe*. J Cell Biol **137,** 1309-1319.

Komatsu, S., Yano, T., Shibata, M., Tuft, R.A., and Ikebe, M. (2000). Effects of the regulatory light chain phosphorylation of myosin II on mitosis and cytokinesis of mammalian cells. J Biol Chem **275,** 34512-34520.

Kosetsu, K., de Keijzer, J., Janson, M.E., and Goshima, G. (2013). MICROTUBULE-ASSOCIATED PROTEIN65 is essential for maintenance of phragmoplast bipolarity and formation of the cell plate in *Physcomitrella patens*. Plant Cell **25,** 4479-4492.

Kumagai, F., Yoneda, A., Tomida, T., Sano, T., Nagata, T., and Hasezawa, S. (2001). Fate of nascent microtubules organized at the M/G1 interface, as visualized by synchronized

tobacco BY-2 cells stably expressing GFP-tubulin: time-sequence observations of the reorganization of cortical microtubules in living plant cells. Plant Cell Physiol **42,** 723-732.

Kwon, C., Neu, C., Pajonk, S., Yun, H.S., Lipka, U., Humphry, M., Bau, S., Straus, M., Kwaaitaal, M., Rampelt, H., El Kasmi, F., Jurgens, G., Parker, J., Panstruga, R., Lipka, V., and Schulze-Lefert, P. (2008). Co-option of a default secretory pathway for plant immune responses. Nature **451,** 835-840.

Lam, S.K., Cai, Y., Tse, Y.C., Wang, J., Law, A.H., Pimpl, P., Chan, H.Y., Xia, J., and Jiang, L. (2009). BFA-induced compartments from the Golgi apparatus and trans-Golgi network/early endosome are distinct in plant cells. Plant J **60,** 865-881.

Lansky, Z., Braun, M., Ludecke, A., Schlierf, M., ten Wolde, P.R., Janson, M.E., and Diez, S. (2015). Diffusible Crosslinkers Generate Directed Forces in Microtubule Networks. Cell **160,** 1159-1168.

Lantz, V.A., and Miller, K.G. (1998). A class VI unconventional myosin is associated with a homologue of a microtubule-binding protein, cytoplasmic linker protein-170, in neurons and at the posterior pole of *Drosophila* embryos. J Cell Biol **140,** 897-910.

Lauber, M.H., Waizenegger, I., Steinmann, T., Schwarz, H., Mayer, U., Hwang, I., Lukowitz, W., and Jurgens, G. (1997). The *Arabidopsis* KNOLLE protein is a cytokinesis-specific syntaxin. J Cell Biol **139,** 1485-1493.

Lee, J.Y., Lee, H.S., Wi, S.J., Park, K.Y., Schmit, A.C., and Pai, H.S. (2009). Dual functions of *Nicotiana benthamiana* Rae1 in interphase and mitosis. Plant J **59,** 278-291.

Lee, Y.R., and Liu, B. (2013). The rise and fall of the phragmoplast microtubule array. Curr Opin Plant Biol **16,** 757-763.

Lipka, V., Kwon, C., and Panstruga, R. (2007). SNARE-ware: the role of SNARE-domain proteins in plant biology. Annu Rev Cell Dev Biol **23,** 147-174.

Liu, B., Cyr, R.J., and Palevitz, B.A. (1996). A kinesin-like protein, KatAp, in the cells of *Arabidopsis* and other plants. Plant Cell **8,** 119-132.

Lloyd, C., and Chan, J. (2006). Not so divided: the common basis of plant and animal cell division. Nat Rev Mol Cell Biol **7,** 147-152.

Lu, C., Reedy, M., and Erickson, H.P. (2000). Straight and curved conformations of FtsZ are regulated by GTP hydrolysis. J Bacteriol **182,** 164-170.

Lucretti, S., and Dolezel, J. (1995). Cell cycle synchronization, chromosome isolation, and flow-sorting in plants. Methods in Cell Biology, Vol 50 **50,** 61-83.

Lutkenhaus, J., and Addinall, S.G. (1997). Bacterial cell division and the Z ring. Annu Rev Biochem **66,** 93-116.

Maiato, H., Rieder, C.L., and Khodjakov, A. (2004). Kinetochore-driven formation of kinetochore fibers contributes to spindle assembly during animal mitosis. J Cell Biol **167,** 831-840.

Masoud, K., Herzog, E., Chaboute, M.E., and Schmit, A.C. (2013). Microtubule nucleation and establishment of the mitotic spindle in vascular plant cells. Plant J **75,** 245-257.

Masuda, H., McDonald, K.L., and Cande, W.Z. (1988). The mechanism of anaphase spindle elongation: uncoupling of tubulin incorporation and microtubule sliding during in vitro spindle reactivation. J Cell Biol **107,** 623-633.

May, K.M., Watts, F.Z., Jones, N., and Hyams, J.S. (1997). Type II myosin involved in cytokinesis in the fission yeast, *Schizosaccharomyces pombe*. Cell Motil Cytoskeleton **38,** 385-396.

McNally, F.J. (1996). Modulation of microtubule dynamics during the cell cycle. Curr Opin Cell Biol **8,** 23-29.

McNally, F.J., and Thomas, S. (1998). Katanin is responsible for the M-phase microtubule-severing activity in *Xenopus* eggs. Mol Biol Cell **9,** 1847-1861.

Mehta, A.D., Rock, R.S., Rief, M., Spudich, J.A., Mooseker, M.S., and Cheney, R.E. (1999). Myosin-V is a processive actin-based motor. Nature **400,** 590-593.

Miki, T., Naito, H., Nishina, M., and Goshima, G. (2014). Endogenous localizome identifies 43 mitotic kinesins in a plant cell. Proc Natl Acad Sci U S A **111,** E1053-1061.

Misumi, Y., Misumi, Y., Miki, K., Takatsuki, A., Tamura, G., and Ikehara, Y. (1986). Novel blockade by brefeldin A of intracellular transport of secretory proteins in cultured rat hepatocytes. J Biol Chem **261,** 11398-11403.

Molchan, T.M., Valster, A.H., and Hepler, P.K. (2002). Actomyosin promotes cell plate alignment and late lateral expansion in *Tradescantia* stamen hair cells. Planta **214,** 683-693.

Mollinari, C., Kleman, J.P., Jiang, W., Schoehn, G., Hunter, T., and Margolis, R.L. (2002). PRC1 is a microtubule binding and bundling protein essential to maintain the mitotic spindle midzone. J Cell Biol **157,** 1175-1186.

Mukherjee, A., Saez, C., and Lutkenhaus, J. (2001). Assembly of an FtsZ mutant deficient in GTPase activity has implications for FtsZ assembly and the role of the Z ring in cell division. J Bacteriol **183,** 7190-7197.

Mukhina, S., Wang, Y.L., and Murata-Hori, M. (2007). Alpha-actinin is required for tightly regulated remodeling of the actin cortical network during cytokinesis. Dev Cell **13,** 554-565.

Muller, S., Wright, A.J., and Smith, L.G. (2009). Division plane control in plants: new players in the band. Trends Cell Biol **19,** 180-188.

Murata, T., and Hasebe, M. (2007). Microtubule-dependent microtubule nucleation in plant cells. J Plant Res **120,** 73-78.

Murata, T., Sano, T., Sasabe, M., Nonaka, S., Higashiyama, T., Hasezawa, S., Machida, Y., and Hasebe, M. (2013). Mechanism of microtubule array expansion in the cytokinetic phragmoplast. Nat Commun **4,** 1967.

Nakamura, M., and Hashimoto, T. (2009). A mutation in the *Arabidopsis* gamma-tubulin-containing complex causes helical growth and abnormal microtubule branching. J Cell Sci **122,** 2208-2217.

Nakaoka, Y., Miki, T., Fujioka, R., Uehara, R., Tomioka, A., Obuse, C., Kubo, M., Hiwatashi, Y., and Goshima, G. (2012). An inducible RNA interference system in *Physcomitrella patens* reveals a dominant role of augmin in phragmoplast microtubule generation. Plant Cell **24,** 1478-1493.

Nebenfuhr, A., Frohlick, J.A., and Staehelin, L.A. (2000). Redistribution of Golgi stacks and other organelles during mitosis and cytokinesis in plant cells. Plant Physiol **124,** 135-151.

Nishihama, R., and Machida, Y. (2001). Expansion of the phragmoplast during plant cytokinesis: a MAPK pathway may MAP it out. Curr Opin Plant Biol **4,** 507-512.

Oda, Y., and Fukuda, H. (2011). Dynamics of *Arabidopsis* SUN proteins during mitosis and their involvement in nuclear shaping. Plant J **66,** 629-641.

Otegui, M.S., Mastronarde, D.N., Kang, B.H., Bednarek, S.Y., and Staehelin, L.A. (2001). Three-dimensional analysis of syncytial-type cell plates during endosperm cellularization visualized by high resolution electron tomography. Plant Cell **13,** 2033-2051.

Panteris, E. (2008). Cortical actin filaments at the division site of mitotic plant cells: a reconsideration of the 'actin-depleted zone'. New Phytol **179,** 334-341.

Panteris, E., Adamakis, I.D., Voulgari, G., and Papadopoulou, G. (2011). A role for katanin in plant cell division: microtubule organization in dividing root cells of fra2 and lue1*Arabidopsis thaliana* mutants. Cytoskeleton **68,** 401-413.

Pastuglia, M., Azimzadeh, J., Camilleri, C., and Bouchez, D. (2003). Forward and reverse genetics in *Arabidopsis*: isolation of cytoskeletal mutants. Cell Biol Int **27,** 249-250.

Peremyslov, V.V., Prokhnevsky, A.I., Avisar, D., and Dolja, V.V. (2008). Two class XI myosins function in organelle trafficking and root hair development in *Arabidopsis*. Plant Physiology **146,** 1109-1116.

Peremyslov, V.V., Klocko, A.L., Fowler, J.E., and Dolja, V.V. (2012). *Arabidopsis* myosin XI-K localizes to the motile endomembrane vesicles associated with F-actin. Frontiers in Plant Science **3,** 184.

Pichoff, S., and Lutkenhaus, J. (2002). Unique and overlapping roles for ZipA and FtsA in septal ring assembly in *Escherichia coli*. Embo J **21,** 685-693.

Pollard, T.D. (2010). Mechanics of cytokinesis in eukaryotes. Curr Opin Cell Biol **22,** 50-56.

Qi, X., and Zheng, H. (2011). *Arabidopsis* TRAPPII is functionally linked to Rab-A, but not Rab-D in polar protein trafficking in trans-Golgi network. Plant Signal Behav **6,** 1679-1683.

Reichardt, I., Stierhof, Y.D., Mayer, U., Richter, S., Schwarz, H., Schumacher, K., and Jurgens, G. (2007). Plant cytokinesis requires de novo secretory trafficking but not endocytosis. Curr Biol **17,** 2047-2053.

Reichelt, S., Knight, A.E., Hodge, T.P., Baluska, F., Samaj, J., Volkmann, D., and Kendrick-Jones, J. (1999). Characterization of the unconventional myosin VIII in plant cells and its localization at the post-cytokinetic cell wall. Plant J **19,** 555-567.

Reichl, E.M., Ren, Y., Morphew, M.K., Delannoy, M., Effler, J.C., Girard, K.D., Divi, S., Iglesias, P.A., Kuo, S.C., and Robinson, D.N. (2008). Interactions between myosin and actin crosslinkers control cytokinesis contractility dynamics and mechanics. Curr Biol **18,** 471-480.

Reisen, D., and Hanson, M.R. (2007). Association of six YFP-myosin XI-tail fusions with mobile plant cell organelles. BMC Plant Biol **7,** 6.

Rensing, S.A., Lang, D., Zimmer, A.D., Terry, A., Salamov, A., Shapiro, H., Nishiyama, T., Perroud, P.F., Lindquist, E.A., Kamisugi, Y., Tanahashi, T., Sakakibara, K., Fujita, T., Oishi, K., Shin, I.T., Kuroki, Y., Toyoda, A., Suzuki, Y., Hashimoto, S., Yamaguchi, K., Sugano, S., Kohara, Y., Fujiyama, A., Anterola, A., Aoki, S., Ashton, N., Barbazuk, W.B., Barker, E., Bennetzen, J.L., Blankenship, R., Cho, S.H., Dutcher, S.K., Estelle, M., Fawcett, J.A., Gundlach, H., Hanada, K., Heyl, A., Hicks, K.A., Hughes, J., Lohr, M., Mayer, K., Melkozernov, A., Murata, T., Nelson, D.R., Pils, B., Prigge, M., Reiss, B., Renner, T., Rombauts, S., Rushton, P.J., Sanderfoot, A., Schween, G., Shiu, S.H., Stueber, K., Theodoulou, F.L., Tu, H., Van de Peer, Y., Verrier, P.J., Waters, E., Wood, A., Yang, L., Cove, D., Cuming, A.C., Hasebe, M., Lucas, S., Mishler, B.D., Reski, R., Grigoriev, I.V., Quatrano, R.S., and Boore, J.L. (2008). The *Physcomitrella* genome reveals evolutionary insights into the conquest of land by plants. Science **319,** 64-69.

Ridge, R.W., Uozumi, Y., Plazinski, J., Hurley, U.A., and Williamson, R.E. (1999). Developmental transitions and dynamics of the cortical ER of *Arabidopsis* cells seen with green fluorescent protein. Plant Cell Physiol **40,** 1253-1261.

Rybak, K., Steiner, A., Synek, L., Klaeger, S., Kulich, I., Facher, E., Wanner, G., Kuster, B., Zarsky, V., Persson, S., and Assaad, F.F. (2014). Plant cytokinesis is orchestrated by the sequential action of the TRAPPII and exocyst tethering complexes. Dev Cell **29,** 607-620.

Sampson, K., and Pickett-Heaps, J.D. (2001). Phallacidin stains the kinetochore region in the mitotic spindle of the green algae *Oedogonium spp*. Protoplasma **217,** 166-176.

Sandquist, J.C., Kita, A.M., and Bement, W.M. (2011). And the dead shall rise: actin and myosin return to the spindle. Dev Cell **21,** 410-419.

Sanger, J.M., and Sanger, J.W. (1980). Banding and polarity of actin filaments in interphase and cleaving cells. J Cell Biol **86,** 568-575.

Sano, T., Higaki, T., Oda, Y., Hayashi, T., and Hasezawa, S. (2005). Appearance of actin microfilament 'twin peaks' in mitosis and their function in cell plate formation, as visualized in tobacco BY-2 cells expressing GFP-fimbrin. Plant J **44,** 595-605.

Sasabe, M., Soyano, T., Takahashi, Y., Sonobe, S., Igarashi, H., Itoh, T.J., Hidaka, M., and Machida, Y. (2006). Phosphorylation of NtMAP65-1 by a MAP kinase down-regulates its activity of microtubule bundling and stimulates progression of cytokinesis of tobacco cells. Genes Dev **20,** 1004-1014.

Schaefer, D.G., and Zryd, J.P. (1997). Efficient gene targeting in the moss *Physcomitrella patens*. Plant Journal **11,** 1195-1206.

Scholey, J.M., Brust-Mascher, I., and Mogilner, A. (2003). Cell division. Nature **422,** 746-752.

Schroeder, T.E. (1973). Actin in dividing cells: contractile ring filaments bind heavy meromyosin. Proc Natl Acad Sci U S A **70,** 1688-1692.

Seagull, R.W., Falconer, M.M., and Weerdenburg, C.A. (1987). Microfilaments: dynamic arrays in higher plant cells. J Cell Biol **104,** 995-1004.

Segui-Simarro, J.M., Austin, J.R., 2nd, White, E.A., and Staehelin, L.A. (2004). Electron tomographic analysis of somatic cell plate formation in meristematic cells of *Arabidopsis* preserved by high-pressure freezing. Plant Cell **16,** 836-856.

Sharp, D.J., Yu, K.R., Sisson, J.C., Sullivan, W., and Scholey, J.M. (1999). Antagonistic microtubule-sliding motors position mitotic centrosomes in *Drosophila* early embryos. Nat Cell Biol **1,** 51-54.

Sluder, G., and Rieder, C.L. (1985a). Experimental separation of pronuclei in fertilized sea urchin eggs: chromosomes do not organize a spindle in the absence of centrosomes. J Cell Biol **100,** 897-903.

Sluder, G., and Rieder, C.L. (1985b). Centriole number and the reproductive capacity of spindle poles. J Cell Biol **100,** 887-896.

Smertenko, A., Saleh, N., Igarashi, H., Mori, H., Hauser-Hahn, I., Jiang, C.J., Sonobe, S., Lloyd, C.W., and Hussey, P.J. (2000). A new class of microtubule-associated proteins in plants. Nature Cell Biology **2,** 750-753.

Smertenko, A.P., Chang, H.Y., Wagner, V., Kaloriti, D., Fenyk, S., Sonobe, S., Lloyd, C., Hauser, M.T., and Hussey, P.J. (2004). The *Arabidopsis* microtubule-associated protein AtMAP65-1: molecular analysis of its microtubule bundling activity. Plant Cell **16,** 2035-2047.

Sommi, P., Cheerambathur, D., Brust-Mascher, I., and Mogilner, A. (2011). Actomyosin-dependent cortical dynamics contributes to the prophase force-balance in the early *Drosophila* embryo. Plos One **6,** e18366.

Sontag, J.M., Nunbhakdi-Craig, V., White, C.L., 3rd, Halpain, S., and Sontag, E. (2012). The protein phosphatase PP2A/Balpha binds to the microtubule-associated proteins Tau and MAP2 at a motif also recognized by the kinase Fyn: implications for tauopathies. J Biol Chem **287,** 14984-14993.

Sparkes, I.A., Teanby, N.A., and Hawes, C. (2008). Truncated myosin XI tail fusions inhibit peroxisome, Golgi, and mitochondrial movement in tobacco leaf epidermal cells: a genetic tool for the next generation. Journal of Experimental Botany **59,** 2499-2512.

Tamura, K., Iwabuchi, K., Fukao, Y., Kondo, M., Okamoto, K., Ueda, H., Nishimura, M., and Hara-Nishimura, I. (2013). Myosin XI-i links the nuclear membrane to the cytoskeleton to control nuclear movement and shape in *Arabidopsis*. Curr Biol **23,** 1776-1781.

Thompson, R.F., and Langford, G.M. (2002). Myosin superfamily evolutionary history. Anat Rec **268,** 276-289.

Tominaga, M., Kojima, H., Yokota, E., Orii, H., Nakamori, R., Katayama, E., Anson, M., Shimmen, T., and Oiwa, K. (2003). Higher plant myosin XI moves processively on actin with 35 nm steps at high velocity. Embo J **22,** 1263-1272.

Vanstraelen, M., Van Damme, D., De Rycke, R., Mylle, E., Inze, D., and Geelen, D. (2006). Cell cycle-dependent targeting of a kinesin at the plasma membrane demarcates the division site in plant cells. Current Biology **16,** 308-314.

Vidali, L., Burkart, G.M., Augustine, R.C., Kerdavid, E., Tüzel, E., and Bezanilla, M. (2010). Myosin XI is essential for tip growth in *Physcomitrella patens*. Plant Cell **22,** 1868-1882.

Volkmann, D., Mori, T., Tirlapur, U.K., Konig, K., Fujiwara, T., Kendrick-Jones, J., and Baluska, F. (2003). Unconventional myosins of the plant-specific class VIII:

endocytosis, cytokinesis, plasmodesmata/pit-fields, and cell-to-cell coupling. Cell Biol Int **27,** 289-291.

Vos, J.W., Dogterom, M., and Emons, A.M. (2004). Microtubules become more dynamic but not shorter during preprophase band formation: a possible "search-and-capture" mechanism for microtubule translocation. Cell Motil Cytoskeleton **57,** 246-258.

Vos, J.W., Safadi, F., Reddy, A.S., and Hepler, P.K. (2000). The kinesin-like calmodulin binding protein is differentially involved in cell division. Plant Cell **12,** 979-990.

Walker, K.L., Muller, S., Moss, D., Ehrhardt, D.W., and Smith, L.G. (2007). *Arabidopsis* TANGLED identifies the division plane throughout mitosis and cytokinesis. Curr Biol **17,** 1827-1836.

Wiedemeier, A.M., Judy-March, J.E., Hocart, C.H., Wasteneys, G.O., Williamson, R.E., and Baskin, T.I. (2002). Mutant alleles of *Arabidopsis* RADIALLY SWOLLEN 4 and 7 reduce growth anisotropy without altering the transverse orientation of cortical microtubules or cellulose microfibrils. Development **129,** 4821-4830.

Wright, A.J., Gallagher, K., and Smith, L.G. (2009). discordia1 and alternative discordia1 function redundantly at the cortical division site to promote preprophase band formation and orient division planes in maize. Plant Cell **21,** 234-247.

Wu, S.Z., and Bezanilla, M. (2014). Myosin VIII associates with microtubule ends and together with actin plays a role in guiding plant cell division. Elife **3**.

Wu, S.Z., Ritchie, J.A., Pan, A.H., Quatrano, R.S., and Bezanilla, M. (2011). Myosin VIII regulates protonemal patterning and developmental timing in the moss *Physcomitrella patens*. Mol Plant **4,** 909-921.

Wu, X., Kocher, B., Wei, Q., and Hammer, J.A., 3rd. (1998). Myosin Va associates with microtubule-rich domains in both interphase and dividing cells. Cell Motil Cytoskeleton **40,** 286-303.

Xie, L., and Forer, A. (2008). Jasplakinolide, an actin stabilizing agent, alters anaphase chromosome movements in crane-fly spermatocytes. Cell Motil Cytoskeleton **65,** 876-889.

Xu, X.M., Zhao, Q., Rodrigo-Peiris, T., Brkljacic, J., He, C.S., Muller, S., and Meier, I. (2008). RanGAP1 is a continuous marker of the *Arabidopsis* cell division plane. Proc Natl Acad Sci U S A **105,** 18637-18642.

Yasuda, H., Kanda, K., Koiwa, H., Suenaga, K., Kidou, S., and Ejiri, S. (2005). Localization of actin filaments on mitotic apparatus in tobacco BY-2 cells. Planta **222,** 118-129.

Yasuhara, H., and Shibaoka, H. (2000). Inhibition of cell-plate formation by brefeldin A inhibited the depolymerization of microtubules in the central region of the phragmoplast. Plant Cell Physiol **41,** 300-310.

Yokota, E., Ueda, H., Hashimoto, K., Orii, H., Shimada, T., Hara-Nishimura, I., and Shimmen, T. (2011). Myosin XI-dependent formation of tubular structures from endoplasmic reticulum isolated from tobacco cultured BY-2 cells. Plant Physiol **156,** 129-143.

Yokota, E., Ueda, S., Tamura, K., Orii, H., Uchi, S., Sonobe, S., Hara-Nishimura, I., and Shimmen, T. (2009). An isoform of myosin XI is responsible for the translocation of endoplasmic reticulum in tobacco cultured BY-2 cells. Journal of Experimental Botany **60,** 197-212.

Yu, M., Yuan, M., and Ren, H. (2006). Visualization of actin cytoskeletal dynamics during the cell cycle in tobacco (*Nicotiana tabacum* L. cv Bright Yellow) cells. Biol Cell **98,** 295-306.

Zhang, H., and Dawe, R.K. (2011). Mechanisms of plant spindle formation. Chromosome Res **19,** 335-344.

Zhang, L., Zhang, H., Liu, P., Hao, H., Jin, J.B., and Lin, J. (2011). *Arabidopsis* R-SNARE proteins VAMP721 and VAMP722 are required for cell plate formation. Plos One **6,** e26129.

Zhou, M., and Wang, Y.L. (2008). Distinct pathways for the early recruitment of myosin II and actin to the cytokinetic furrow. Mol Biol Cell **19,** 318-326.

Zhu, C., and Dixit, R. (2012). Functions of the *Arabidopsis* kinesin superfamily of microtubule-based motor proteins. Protoplasma **249,** 887-899.

7. APPENDIX FOR MEDIUM

7.1.Stock Solutions

	FW	1X	500X	Final Volume	Weight
$MgSO_4 \cdot 7H_2O$	246.48 g/mol	1 mM	500 mM	500 mL	61.6 g
KH_2PO_4	136.09 g/mol	1.84 mM	920 mM	500 mL	62.6 g
$Ca(NO_3)_2 \cdot 4H_2O$	236.15 g/mol	3.4 mM	1700 mM	500 mL	200.7 g
Di-ammonium tartrate	184.15 g/mol	2.72 mM	1360 mM	500 mL	125 g

Micro elements	FW	1X	1000X	Final Volume	Weight
H_3BO_3	61.83 g/mol	9.93 µM	9.93 mM		614 mg
$CuSO_4 \cdot 5H_2O$	249.68 g/mol	220 nM	220 µM		55 mg
$MnCl_2 \cdot 4H_2O$	197.91 g/mol	1.97 µM	1.97 mM		390 mg
$CoCl_2 \cdot 6H_2O$	237.93 g/mol	230 nM	230 µM	1L	55 mg
$ZnSO_4 \cdot 7H_2O$	287.54 g/mol	190 nM	190 µM		55 mg
KI	166 g/mol	168 nM	168 µM		28 mg
$NaMoO_4 \cdot 2H_2O$	241.95 g/mol	100 nM	100 µM		24 mg

	FW	Final Concentration	Final Volume	Weight
$CaCl_2$	147.02 g/mol	1 M	200 mL	29.4 g
Mannitol	182.17 g/mol	0.8 M	500 mL	72.9 g
MES *Adjust pH 5.7 with KOH	195.24 g/mol	20 mM	500 mL	1.95 g
$MgCl_2$	203.3 g/mol	150 mM	500 mL	15.25 g
NaCl	58.44 g/mol	500 mM	500 mL	14.61 g
KCl	74.6 g/mol	50 mM	500 mL	1.86 g

7.2.PpNH_4 Medium 1X

Recipe for 1L:

$MgSO_4 \cdot 7H_2O$ – 500X	2 mL
KH_2PO_4 – 500X	2 mL
$Ca(NO_3) \cdot 4H_2O$ – 500X	2 mL
Di-ammonium tartrate	0.5 g
$FeSO_4 \cdot 7H_2O$	12.5mg
Micro elements 1000X	1 mL
H_2O	Up to 1L

If making solid medium add Agar directly to bottle 7g/1L
Autoclave 20 minutes 121°C

7.3.PpNO_3 Medium 1X

Recipe for 1L:

$MgSO_4 \cdot 7H_2O$ – 500X	2 mL
KH_2PO_4 – 500X	2 mL
$Ca(NO_3) \cdot 4H_2O$ – 500X	2 mL
$FeSO_4 \cdot 7H_2O$	12.5mg
Micro elements 100X	1 mL
H_2O	Up to 1L

If making solid medium add Agar directly in the bottle 7-10g/1L
Autoclave 20 minutes 121°C

7.4.PRM-B 1X

Recipe for 1L:

$MgSO_4 \cdot 7H_2O$ – 500X	2 mL
KH_2PO_4 – 500X	2 mL
$Ca(NO_3) \cdot 4H_2O$ – 500X	2 mL
Di-ammonium tartrate	0.5 g
$FeSO_4 \cdot 7H_2O$	12.5mg
Micro elements 1000X	1 mL
Mannitol	60g
H_2O	Up to 1L

Add Agar directly in the bottle 8g/1L and autoclave 20 minutes 121°C
When medium cools down, add 10mL of 1M $CaCl_2$ stock and then pour plates

7.5.PRM-T 1X

Recipe for 1L:

$MgSO_4 \cdot 7H_2O$ – 500X	2 mL
KH_2PO_4 – 500X	2 mL
$Ca(NO_3) \cdot 4H_2O$ – 500X	2 mL
Di-ammonium tartrate – 500X	2 mL
$FeSO_4 \cdot 7H_2O$	12.5mg
Micro elements 1000X	1 mL
Mannitol	60g
H_2O	Up to 1L

Add Agar directly in the bottle 6g/1L and autoclave 20 minutes 121°C, aliquot by 50mL/bottle
Before use, melt medium and when medium cools down, add 0.5 mL of 1M $CaCl_2$ stock per bottle

7.6.MMg Buffer

Recipe for 100 mL:

	Stock	Final Concentration	Final Volume
Mannitol	0.8 M	0.4 M	50 mL
$MgCl_2$	150 mM	15 mM	10 mL
MES	20 mM pH 5.7	4 mM	20 mL
H_2O			20 mL

7.7.W5 Buffer

Recipe for 100 mL:

	Stock	Final Concentration	Final Volume
NaCl	500 mM	154 mM	30.8 mL
$CaCl_2$	1M	125 mM	12.5 mL
KCl	50 mM	5 mM	10 mL
MES	20 mM pH 5.7	2 mM	10 mL
H_2O			36.7 mL